Abdominal Imaging

Published online: 1 October 2014

Abdom Imaging (2015) 40:875–906
DOI: 10.1007/s00261-014-0250-6

Primary cystic peritoneal masses and mimickers: spectrum of diseases with pathologic correlation

María Arraiza,[1] Ur Metser,[1] Rajkumar Vajpeyi,[2] Korosh Khalili,[1] Anthony Hanbidge,[1] Erin Kennedy,[3] Sangeet Ghai[1]

[1]Joint Department of Medical Imaging, University Health Network - Mount Sinai Hospital - Women's College Hospital, University of Toronto, 585 University Avenue, Toronto, ON M5G 2N2, Canada
[2]Department of Pathology, University Health Network, University of Toronto, 200 Elizabeth Street, Toronto, ON M5G 2C4, Canada
[3]Department of General Surgery, Mount Sinai Hospital, University of Toronto, 600 University Ave, Toronto, ON M5G 1X5, Canada

Abstract

Cystic lesions within the peritoneum have been classified classically according to their lining on histology into four categories—endothelial, epithelial, mesothelial, and others (germ cell tumors, sex cord gonadal stromal tumors, cystic mesenchymal tumors, fibrous wall tumors, and infectious cystic peritoneal lesions). In this article, we will proceed to classify cystic peritoneal lesions focusing on the degree of radiological complexity into three categories—simple cystic, mildly complex, and cystic with solid component lesions. Many intra-abdominal collections within the peritoneal cavity such as abscess, seroma, biloma, urinoma, or lymphocele may mimic primary peritoneal cystic masses and need to be differentiated. Clinical history and imaging features may help differentiate intra-abdominal collections from primary peritoneal masses. Lymphangiomas are benign multilocular cystic masses that can virtually occur in any location within the abdomen and insinuate between structures. Ultrasound may help differentiate enteric duplication cysts from other mesenteric and omental cysts in the abdomen. Double-layered wall along the mesenteric side of bowel may suggest its diagnosis in the proper clinical setting. Characteristic imaging features of hydatid cysts are internal daughter cysts, floating membranes and matrix, peripheral calcifications, and collagenous pericyst. Non-pancreatic psuedocysts usually have a fibrotic thick wall and chylous content may lead to a fat-fluid level. Pseudomyxoma peritonei appears as loculated fluid collections in the peritoneal cavity, omentum, and mesentery and may scallop visceral surfaces. Many of the primary cystic peritoneal masses have specific imaging features which can help in accurate diagnosis and management of these entities. Knowledge of the imaging spectrum of cystic peritoneal masses is necessary to distinguish from other potential cystic abdominal mimicker masses.

Key words: Cystic peritoneal lesions—Lymphangioma—Duplication enteric cyst—Hydatid cyst—Pseudomyxoma peritonei—Non-pancreatic pseudocyst

Cystic peritoneal lesions within the abdominal cavity, either primary or secondary, have to be accurately diagnosed for proper management. When diagnosing a peritoneal mass the first step is to differentiate between a cystic and a solid lesion. At the same time, it is important to determine the organ of origin, and if does not arise from an abdominopelvic solid organ, probably it will originate from the mesentery or omentum.

Classically cystic peritoneal lesions have been classified according to their lining at histology into four categories—endothelial, epithelial, mesothelial, and others [1]. In this article, however, we put forward a new classification according to the radiological complexity of the cystic component of the lesions and discuss their characteristic imaging features with pathologic correlation. Radiological features that help differentiate cystic peritoneal masses from intra-abdominal processes that may mimic primary peritoneal cystic lesions will also be detailed. Each entity is

Correspondence to: Sangeet Ghai; *email:* sangeet.ghai@uhn.ca

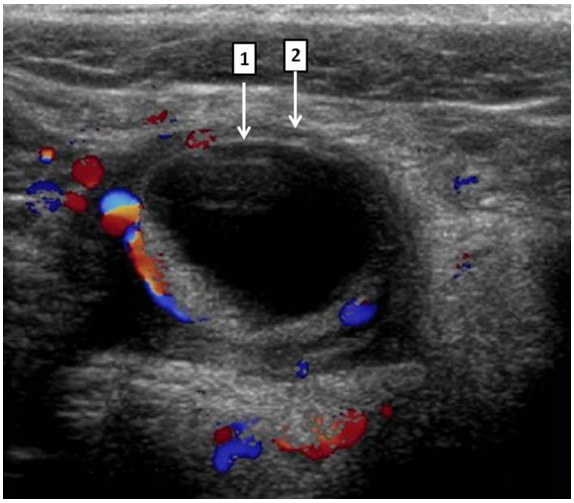

Fig. 1. Duplication cyst in a newborn (double-wall sign). Transverse sonogram reveals an anechoiec, unilocular, thick-walled cyst in the mid abdomen. Echogenic inner mucosal layer (*1*) is seen surrounded by a hypoechoiec muscular layer (*2*) giving a double-layered wall.

described with a summary of the key imaging features when using ultrasonography (US), computed tomography (CT), and magnetic resonance (MR) imaging.

Primary cystic peritoneal lesions

Classification according to the complexity of the cystic component

Cystic masses of the peritoneum can be classified according to the imaging features (degree of complexity of the cystic component) into three categories: simple cystic, mildly complex, and cystic with solid component.

Simple cystic

Enteric duplication cysts and enteric cysts. Enteric duplication cyst is an uncommon congenital abnormality. They have an enteric mucosal lining and double-muscle lining with neural elements (reduplication of the bowel wall) as opposed to an enteric cyst which has a mucosal lining without the muscle layer [2]. They can occur

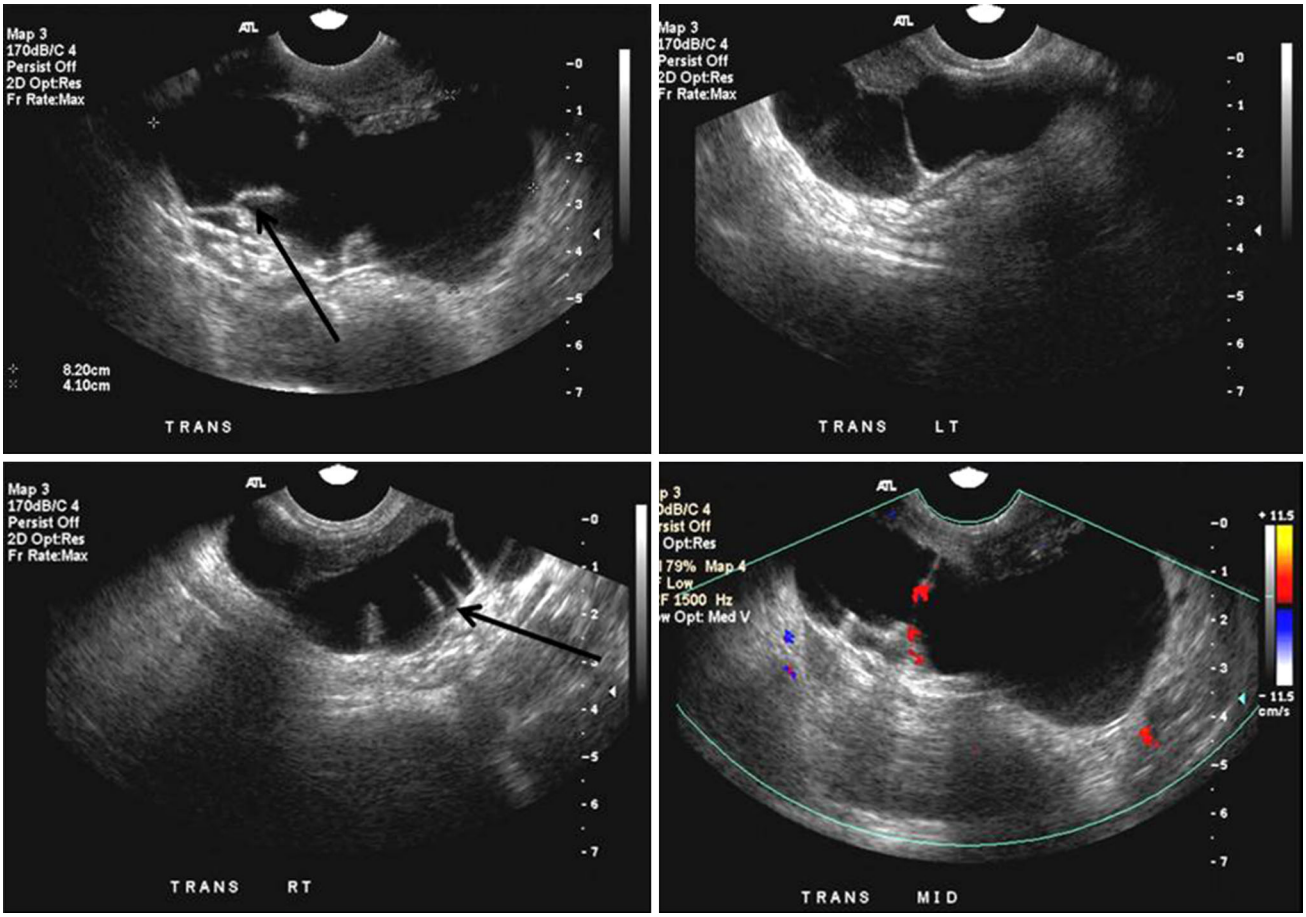

Fig. 2. Duplication cyst in cul de sac (no double-wall sign). Transverse sonogram reveals an anechoic, tubular cystic structure within the pelvic cul-du-sac. There is evidence of thin incomplete internal septations (*arrow*). The wall is apparently simple and thin, without identifying the double-wall sign.

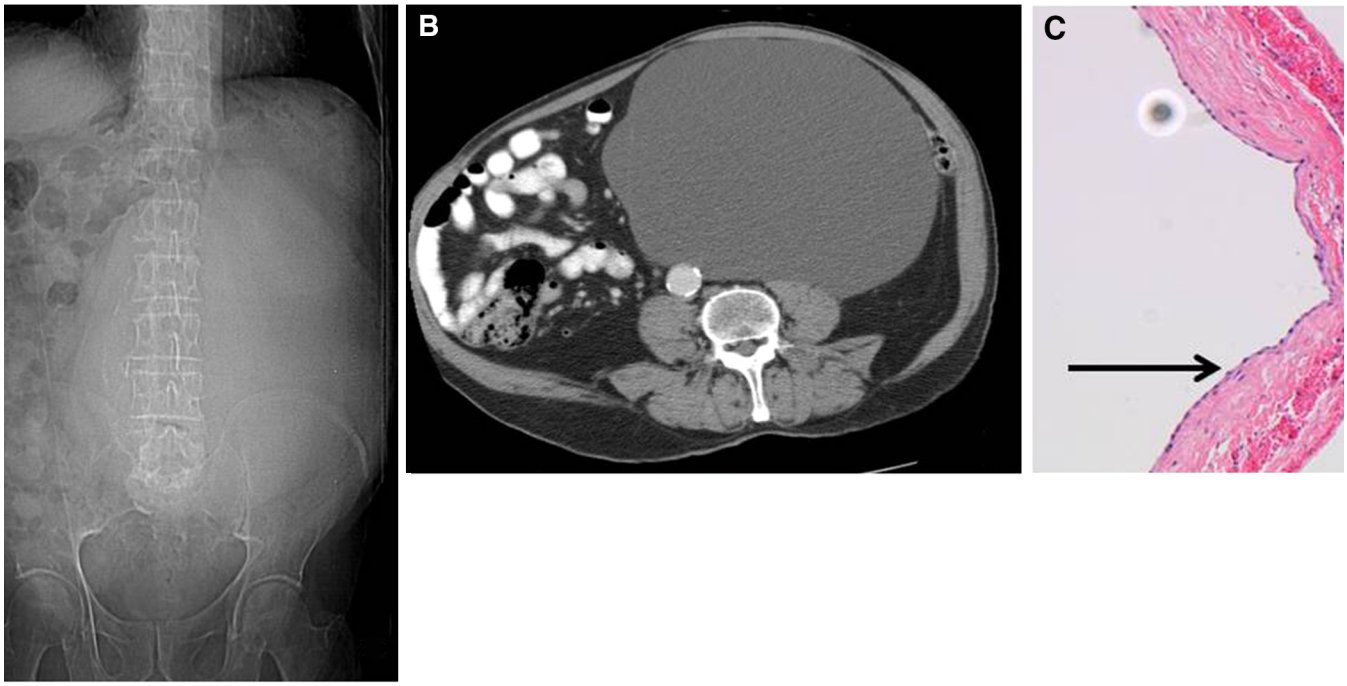

Fig. 3. Simple mesothelial cyst. **A** Abdominal plain film showing a round large mass occupying left mid abdomen. **B** Axial contrast-enhanced CT shows a well-defined cystic mass in the left midabdomen displacing bowel loops to the right, avascular and thin walled. No solid component is noted within the lesion. **C** (H&E stain, ×10): cyst with flattened mesothelial lining (*arrow*) and fibrocollagenous tissue in its wall.

anywhere along the digestive tract on the mesenteric side [3]. Ileum is the commonest site and most manifest in the first year of life. The etiology of duplication cysts is uncertain. Persistent embryonic diverticulum, ischemia [4], and faulty bowel recanalisation [5] have been suggested. Duplication cysts may present with abdominal distention, vomiting, bleeding, or a palpable abdominal mass in children. Complications include perforation, intussusceptions, bowel obstruction, volvulus, and associated malignancy [6]. Duplication cysts may be associated with other vertebral or urogenital malformations [7]. Rarely, enteric duplications cysts may act as lead point for an intussusception. Gastric mucosa may be present in 17%–36% of enteric duplication cysts [8–10] and therefore should be considered as a differential diagnosis in children with gastrointestinal bleeding. Tc-99m pertechnetate radionuclide scan may show tracer uptake within the ectopic gastric mucosa of the mass [11].

US is the first choice diagnostic modality, being duplication enteric cysts characteristically unilocular, thick-walled cysts with evidence of visualization of an echogenic inner mucosal layer surrounded by a hypoechoic outer muscular layer (Fig. 1). This double-layered wall is not always circumferential (Fig. 2) and usually found in over 50% of cases [12]. At CT and MRI a duplication enteric cyst will appear as non-enhancing cystic mass with central values of attenuation and signal intensity of simple fluid, respectively. However, sometimes the mass can show higher attenuation values due to internal hemorrhage or proteinaceous content.

Enteric cysts are lined with gastrointestinal mucosa differing from duplication cysts because there is no reduplication of the bowel wall [2]. Enteric cysts result from migration of a small bowel or colonic diverticulum into the mesentery or the mesocolon [1]. Sonographically, enteric cysts are thin-walled unilocular cysts within the mesentery or the mesocolon.

Mesothelial cysts. Mesothelial cysts are usually located in the small bowel, mesentery, and the mesocolon and are the result of mesothelial-lined peritoneal surfaces failing to coalescence [1]. Sonographically, they are anechoiec, thin-walled, and without internal septations which are an important feature to differentiate mesothelial cysts from lymphangiomas (usually with internal septations). On CT and MR, they have a simple cystic appearance (Fig. 3). Pathologically, they are thin-walled unilocular cysts with mesothelial cells lining the inner surface of the cyst (Fig. 3C) and containing serous material [2].

Mildly complex cystic lesions

Lymphangioma

Lymphangiomas are uncommon benign lymphatic lesions that may occur in many anatomic locations. They occur more commonly in children though adult clinical

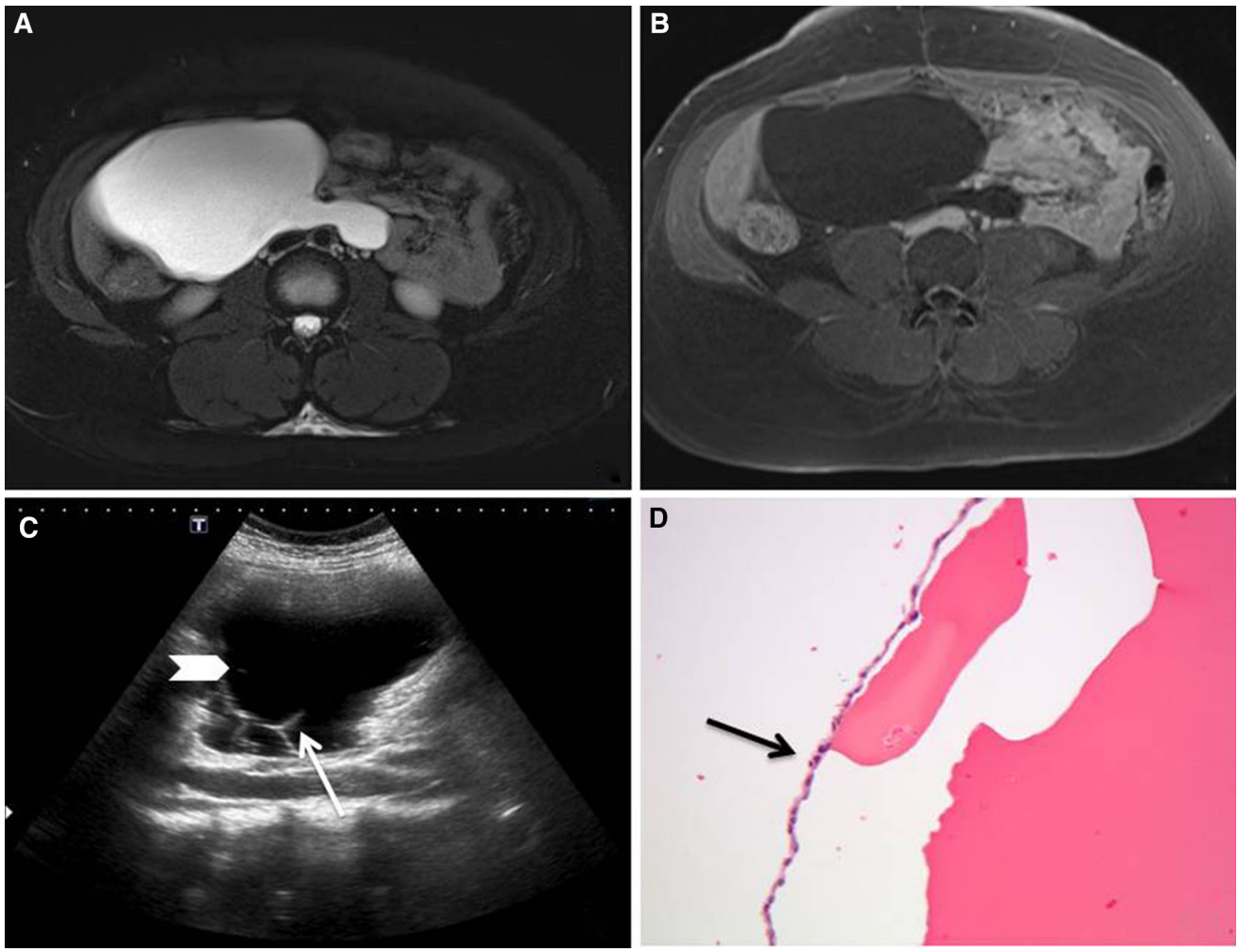

Fig. 4. Mesenteric lymphangioma. **A** Axial T2-weighted MR image shows a high signal lymphangioma within the mesentery. **B** Axial T1-weighted MR image shows a low-signal lymphangioma within the mesentery. **C** Transverse US of the right abdomen shows a multiloculated cystic mass with multiple thin septa (*arrow*) and mild echogenic debris (*arrowhead*). **D** (H&E stain, ×40): cyst lined by flattened endothelium (*arrow*), filled with homogenous eosinophilic material representing lymph.

presentation is not rare [13]. Most of the lymphangiomas occur in the neck (95%) and axillary regions and only 5% are located in the mesentery, retroperitoneum, abdominal viscera, lung, and mediastinum [14].

Lymphangiomas have an insinuating nature making complete surgical excision difficult in some cases. Differentiating abdominal lymphangiomas from other fluid containing masses and ascites in the abdomen is crucial. Septa, compression effect on adjacent intestinal loops and lack of fluid in the dependent recesses of the peritoneum such as paracolic gutters, subhepatic spaces, cul de sac, and between the leaves of the small bowel mesentery [14] are important clues to differentiate lymphangiomas from ascites. Lymphangiomas tend to compress all intra-abdominal organs and unlike ascitis, do not pool in recesses of small bowel mesentery and subhepatic spaces.

Mesenteric lymphangiomas (Figs. 4, 5) are the most common lymphangiomas within the abdomen. Retroperitoneal lymphangiomas are usually large cystic elongated lesions that can cross from one compartment of the retroperitoneum to an adjacent one [15]. Lymphangiomas are infrequently located in the small and large intestine (Fig. 6). They are discovered incidentally at endoscopy or on radiologic studies performed for other reasons [16] though rarely may present with abdominal pain or acutely secondary to volvulus [17]. Primary solid or hollow organ abdominal organ lymphangiomas are rare. They may occur in isolation, or as part of systemic lymphangiomatosis. Splenic lymphangiomas tend to occur in subcapsular locations, secondary to the anatomic distribution of splenic lymphatics. Lymphangiomas of the gallbladder (Fig. 7) are rare and often seen as multilocular cystic masses surrounding the gallbladder. They

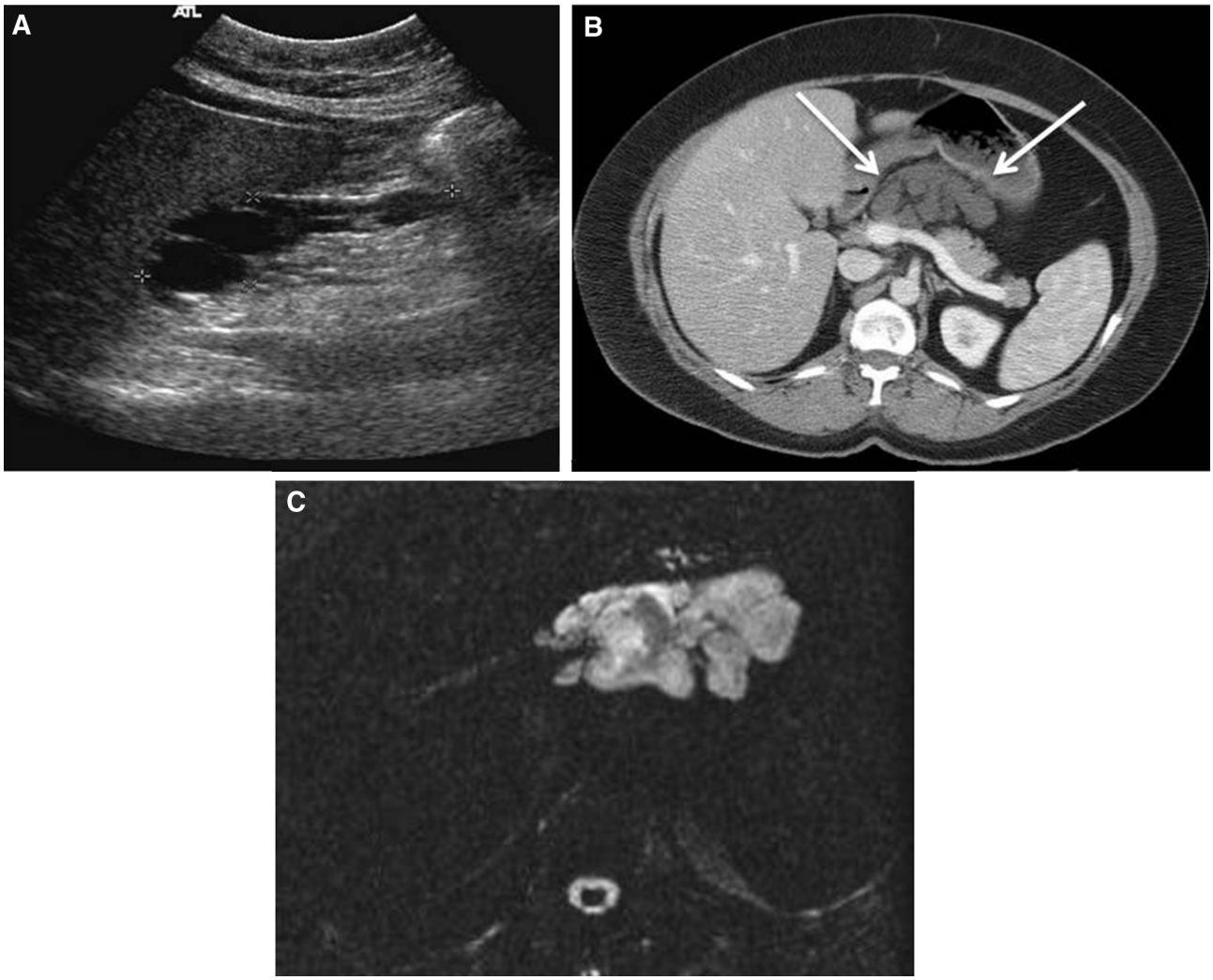

Fig. 5. Mesenteric lymphangioma. **A** Transverse US of the upper abdomen showing a lobulated cystic mass with internal septations. **B** Axial contrast-enhanced CT image shows cystic mesenteric mass anterior to the pancreas (*arrows*). **C** Axial T2-weighted MR image shows a high signal lobulated mass.

are incidentally discovered or the patient may present with biliary colic secondary to mass effect on the cystic duct. There is no communication between the biliary tract and lymphangioma.

Pathologically, lymphangiomas are large multiloculated and thin-walled neoplasms. The fluid contents of lymphangiomas are predominantly chylous, but may be serous or hemorrhagic [2]. Histologically (Fig. 4D), dilated lymphatic spaces are lined with attenuated endothelial cells [13]. Lymphangiomas are locally infiltrative and tend to grow slowly along tissue planes [18].

Lymphangiomatosis (Figs. 8, 9) is a rare disease with multifocal sites of lymphatic proliferation that typically presents during childhood and may involve multiple parenchymal organs including the lung, liver, spleen, bone, and skin.

On US, lymphangiomas are most often multiloculated cystic masses that are usually anechoic or may contain internal echoes or sedimentation, with fluid–fluid levels caused by debris [19] (Figs. 4C, 5A). On CT lymphangiomas are cystic masses, with attenuation values of water (Fig. 5B) if the content is serous, and fat values if the content is chylous [15]. Hemorrhagic content with high attenuation on CT and calcifications are uncommon features [20]. After administration of intravenous contrast lymphangiomas may show enhancement of the cyst wall and septa. On MRI, lymphangiomas have low-signal intensity on T1-weighted images and high signal intensity on T2-weighted images, similar to signal intensity of fluid (Fig. 4A, B). In the presence of chyle, signal drop (Fig. 10) may be seen in the opposed-phase chemical shift MR images [21]. If hemorrhage or infec-

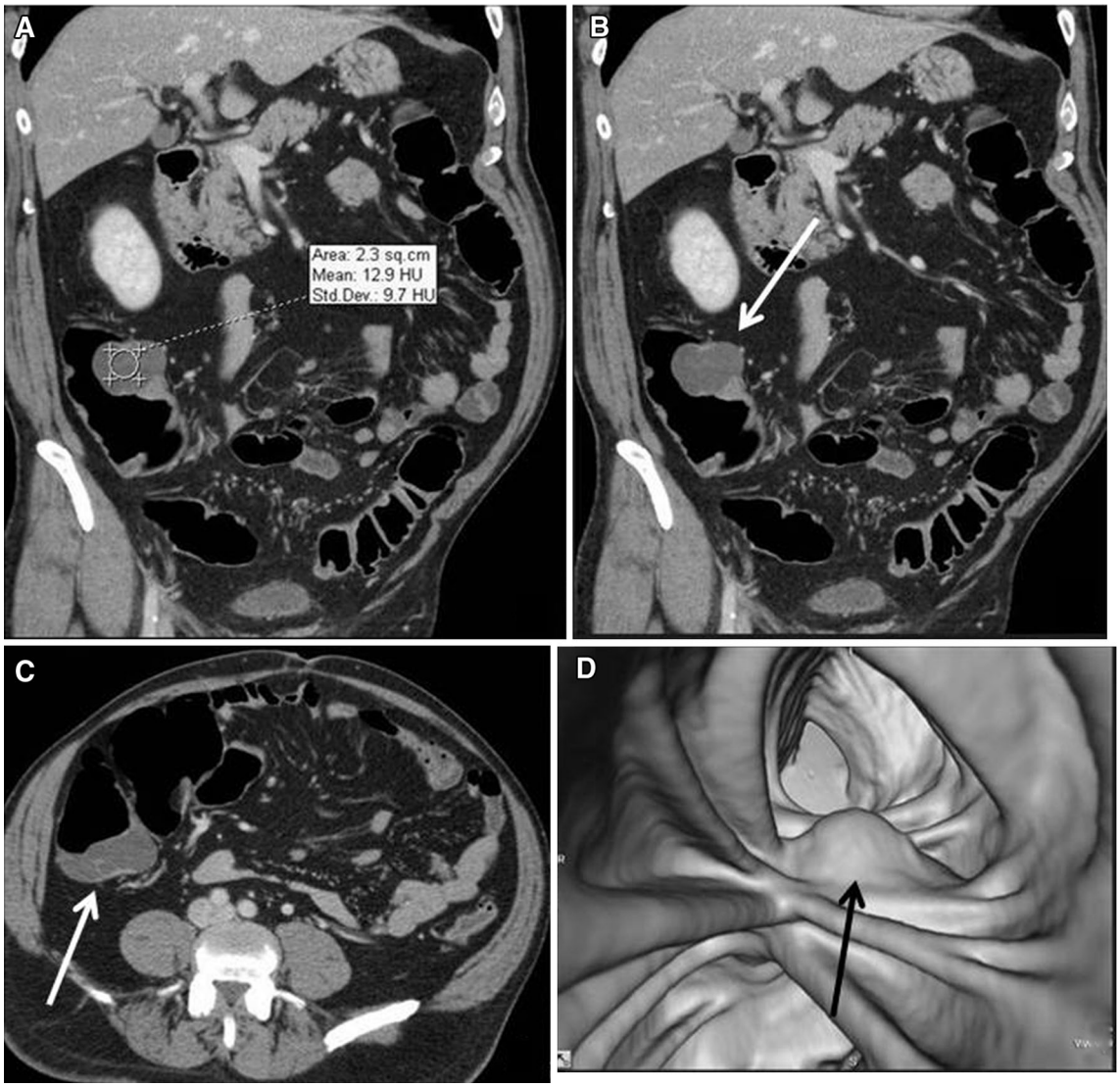

Fig. 6. Colonic lymphangioma. **A**, **B** Coronal contrast-enhanced CT image shows fluid attenuation mural mass (*arrow*) in the right colon. **C** Axial contrast-enhanced CT image shows fluid attenuation mural mass (*arrow*) in the posterior aspect of the right colon. **D** Endoluminal 3D CT colonographic image shows a lobulated mass in the ascending colon (*arrow*).

tion occurs within the lesion, the appearance on CT and MRI can be altered with the lesion appearing more solid [20].

Intestinal lymphangiectasia is a rare disease characterized by severe edema, thickening of the small bowel wall, protein-losing enteropathy, ascitis, and pleural effusion [22]. Intestinal lymphangiectasia may be generalized or localized, depending on the site of blockage of mesenteric lymphatic drainage [23] and can be primary, resulting from congenital lymphatic blockage, or secondary, from inflammatory or neoplastic involvement of the lymphatic system. Typical CT appearance shows diffuse nodular thickening of the small bowel associated with ascitis (Fig. 11) and pleural effusion [24].

Pseudomyxoma peritonei

The term *pseudomyxoma peritonei* refers to the accumulation of gelatinous material on intraperitoneal surfaces due to rupture of a benign or malignant mucin-producing tumor of the appendix, ovary (Fig. 12), pancreas, stomach, colorectum (Fig. 13), or urachus [25]. Histologically, pseudomyxoma peritonei usually arises from mucin-producing cells within well-differentiated columnar epithelium, and are of low grade malignancy [26] (Fig. 13C).

On US, pseudomyxoma peritonei appears as echogenic avascular peritoneal masses or ascites with echogenic particles which do not move (unlike other forms of

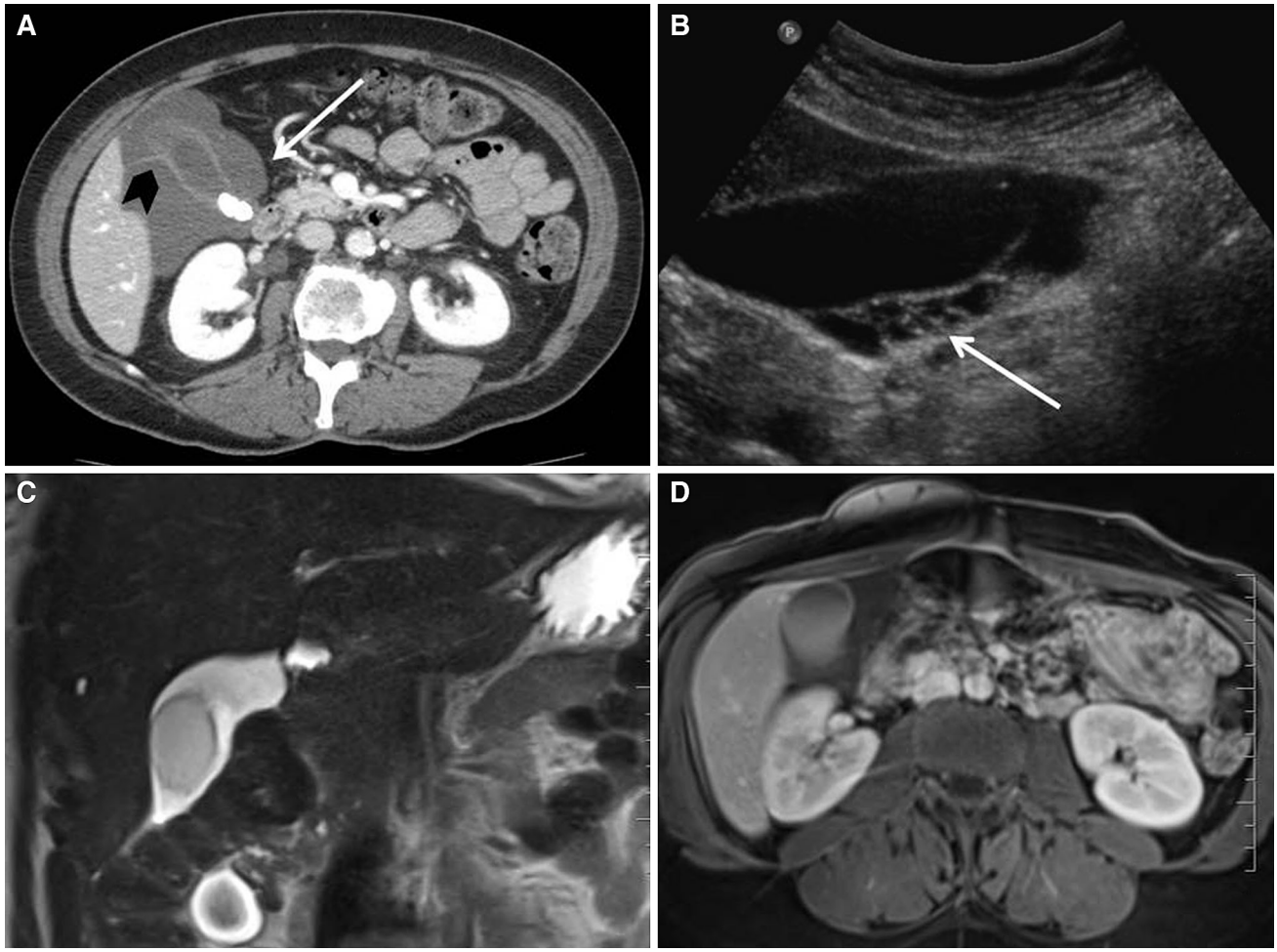

Fig. 7. Gallbladder lymphangioma. **A** Axial contrast-enhanced CT image shows a cystic polylobulated mass surrounding the gallbladder (*arrow*). Note a thin septa within the cystic mass (*arrowhead*). Cholelitiasis are noted within the gallbladder lumen. **B** US of the gallbladder shows a cystic mass surrounding the gallbladder, containing internal septations (*arrow*). **C** Coronal T2-weighted MR image shows a hyperintense cystic mass surrounding the gallbladder. **D** Axial T1-weighted post-contrast image shows a non-enhancing T1 hypointense mass surrounding the gallbladder.

particulate ascites such as hemoperitoneum or pus in the peritoneum) [27] and tend to displace the small bowel loops medially. On CT, it appears as low attenuation and often loculated fluid (Figs. 12, 13) throughout the peritoneum, omentum, and mesentery and may scallop visceral surfaces, particularly the liver [28], a feature which differentiates it from serous ascites. Scattered calcifications may be frequently present. On MRI, pseudomyxoma peritonei has a variable signal intensity depending on the mucin content (Fig. 14). Watery mucin have lower signal intensity on T1-weighted images and higher signal intensity on T2-weighted images; whereas loculi containing thicker mucin have a higher signal intensity on T1 and lower signal intensity on T2-weighted images.

The most common clinical presentation of pseudomyxoma peritonei is abdominal pain, abdominal distension, weight loss as well as new onset of hernia. The natural history of the disease usually is slowly progressive, bowel obstruction being one of the most common complications. Peritoneal metastases may appear as nodular deposits or may be sheath-like, simulating mesothelioma. They are often associated with ascites which at times may be loculated [29] appearing as a cystic peritoneal mass.

Cystadenomas

Both cystadenomas and cystadenocarcinomas may arise from the ovary, pancreas, or appendix and may appear cystic. There are some imaging features that are more suggestive of either benignity or malignancy [30–33]. Entirely cystic component, a thin wall, lack of internal structure as well as lack of papillary projections and the absence of both ascites and peritoneal disease are features that suggest benignity.

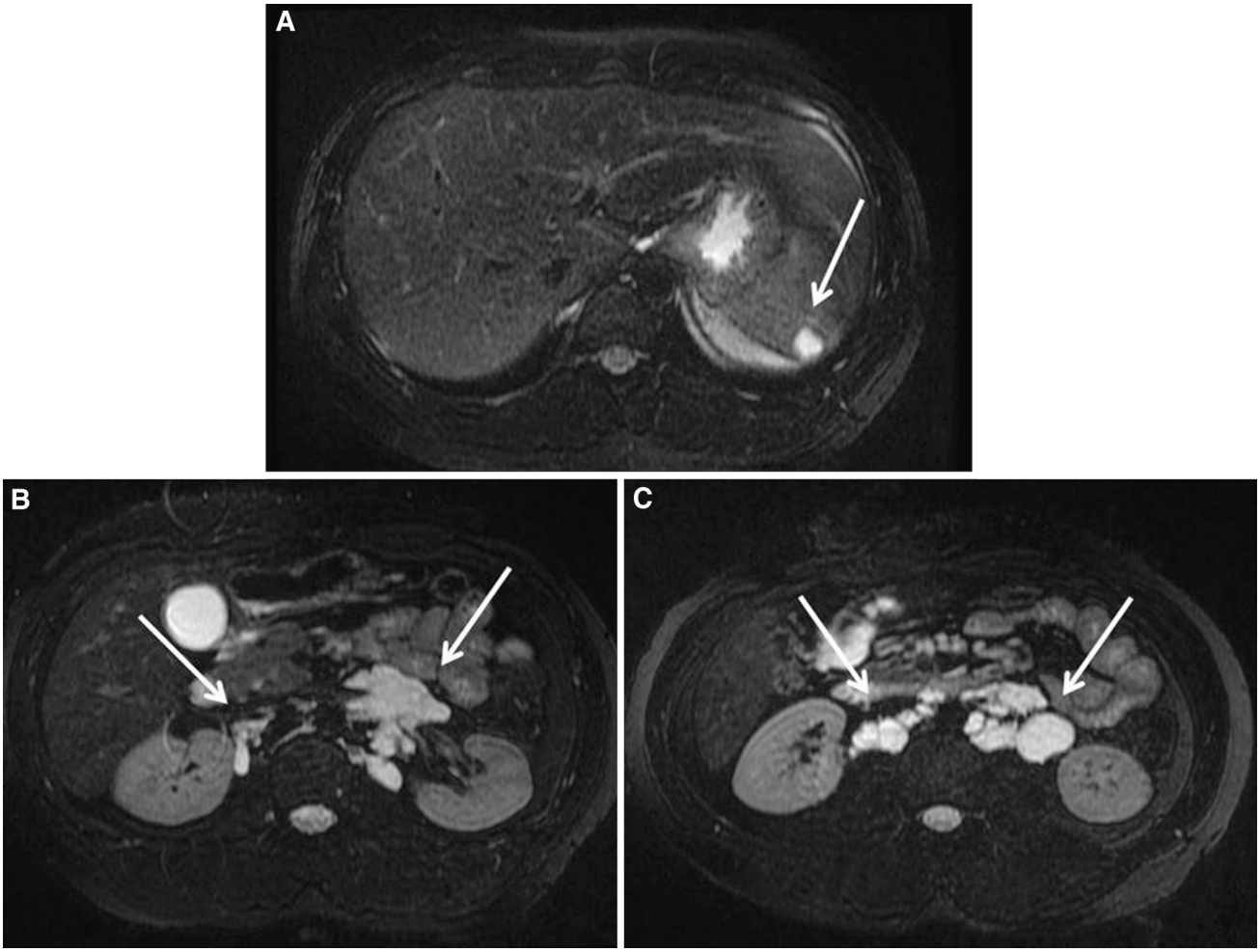

Fig. 8. Diffuse lymphangiomatosis Axial T2-weighted MR image shows diffuse lymphangiomatosis. Multiple cystic polylobulated masses (*arrows*) involving the spleen (**A**) and the retroperitoneum (**B**, **C**) are noted.

The two most common ovarian epithelial neoplasms are serous and mucinous tumors [31]. Serous tumors are the most common subtype of neoplasms in both the benign and malignant category.

There are certain imaging features that can differentiate mucinous from serous tumors. At CT and MRI, a cystic mass that shows homogeneous water attenuation or signal intensity values favors a serous neoplasm. However, a lesion which contains liquids of different attenuation or signal intensity values is most likely mucinous in content due to proteinaceous, mucinous, or hemorrhagic contents (Figs. 15, 16). Psammomatous calcifications (Fig. 17) are more commonly associated with serous content tumors and are seen at histologic analysis in up to 30% of malignant serous tumors [30].

Benign cystic mesothelioma or peritoneal inclusion cyst

Peritoneal inclusion cyst is an unusual multilocular benign cystic pelvic tumor secondary to non-neoplastic reactive mesothelial proliferation which occurs almost exclusively in premenopausal female who have active ovaries and pelvic adhesions with impaired absorption of peritoneal fluid secondary to pelvic surgery, pelvic trauma, endometriosis, or pelvic inflammatory disease. When they occur in men, although very rare, benign cystic mesothelioma arises from the peritoneal surface along the superior margin of the bladder or in the retrovesical space. Pathologically benign cystic mesothelioma is composed of multiple, translucent, fluid-filled cysts that grow along the pelvic peritoneum [34], are thin-walled and histologically are lined by flattened or cuboidal mesothelial cells. The most common clinical scenario is chronic or intermittent lower abdominal or pelvic pain. Other signs and symptoms include abdominal distension, tenderness, palpable abdominal mass, dyspareunia, constipation and urinary hesitancy, and frequency [35, 36].

On US peritoneal inclusion cysts are usually anechoic multiseptated cystic masses adherent to normal or distorted ovaries (Fig. 18). Peritoneal inclusion cysts may

Fig. 9. Diffuse lymphangiomatosis. **A** Axial T2-weighted MR image and **B** coronal contrast-enhanced CT show diffuse lymphangiomatosis. Multiple cystic polylobulated masses involving the spleen and the retroperitoneum are noted.

completely surround ovaries such that the ovaries appear entrapped within the lesion [37] but do not involve the ovarian parenchyma. The fluid within the cysts may contain echoes from debris or hemorrhage. Nodular excrescences or thick, polypoid, and incomplete septations may be present simulating an ovarian neoplasm [34]. Low-resistance flow can be detected within the septations due to vessels running in the mesothelial tissue. On CT peritoneal inclusion cysts have usually fluid attenuation values and the septa enhance after intravenous contrast and have no calcifications. If hemorrhage is present within the cyst, density of the fluid may be higher. CT may better depict the extent of the process, which when large may extend to the upper abdomen. MR is an excellent technique to assess the anatomic relation of the mass with pelvic structures. On MR, the cyst typically has signal intensity of water (Fig. 19) and septal enhancement is common.

Cystic teratoma

Cystic teratoma (mature), also referred as dermoid cyst, are benign neoplasms that can occur in many locations, but are most commonly seen in gonads, head and neck, anterior mediastinum, sacrococcygeal area, retroperitoneum, and central nervous system. Dermoids have been described throughout the gastrointestinal tract and intra-abdominal organs including cecum [38], rectum [39], and pancreas [40] and rarely, they may occur in the mesentery or omentum, primarily in pediatric patients. Pathologically, it is a tumor composed of well-differentiated derivations from at least two of the three germ cell layers. Histologically squamous epithelium lines the wall of the cyst and compressed ovarian stroma covers the external surface. Hair follicles, skin glands, muscle, and other tissues lie within the wall (Fig. 20). These tumors usually are incidentally found in asymptomatic patients in the ovary and when present, most common symptoms are abdominal pain, mass, swelling, and abnormal uterine bleeding.

On US, cystic teratomas are anechoic and well-defined cystic lesions which may contain peripheral echogenic foci with acoustic shadowing, due to calcifications and may contain some echogenic material within, corresponding to fat (Fig. 21A). On CT, fat attenuation values (−90 to −130 HU) within a cyst is diagnostic of cystic teratoma. On MR, the presence of suppression of high signal intensity sebum/fat on T1-weighted images with frequency selective fat saturation sequences as well as signal drop in the opposed-phase chemical shift MR images within these cysts, is easily appreciated and diagnostic for mature teratoma (Fig. 21C, D).

Immature teratoma is the malignant form of teratoma that contains immature or embryonic tissues. The tumor presents as a large heterogeneous mass with areas of low-attenuation fat, enhancing soft tissue component, and high-attenuation calcification (Fig. 22).

Intraperitoneal pseudocysts

Non-pancreatic pseudocysts are rare lesions that usually arise from the mesentery and omentum [1, 41] and are thought to be a sequelae or liquefaction in a hematoma or an abscess that failed to reabsorb completely [1]. They have a fibrotic thick wall composed of fibrous tissue and may present calcifications and inflammatory changes. They are usually septated and contain hemorrhage, pus, serous, or occasionally chylous content fluid [2, 42, 43]. Non-pancreatic pseudocysts usually develop secondary to trauma, surgery, or infection and when symptomatic abdominal pain, nausea, and vomiting are the most common reported symptoms [42].

On US, non-pancreatic pseudocysts demonstrate intracystic echogenic debris and thick walls. On CT and MRI, they are thick-walled cystic masses (Fig. 23) that may contain fluid–fluid level secondary to hemorrhagic, pus, or chylous content. While the non-dependent portion of the cyst shows fat density, the dependent portion demonstrates water density. MRI using either frequency selective fat saturation or chemical shift imaging can

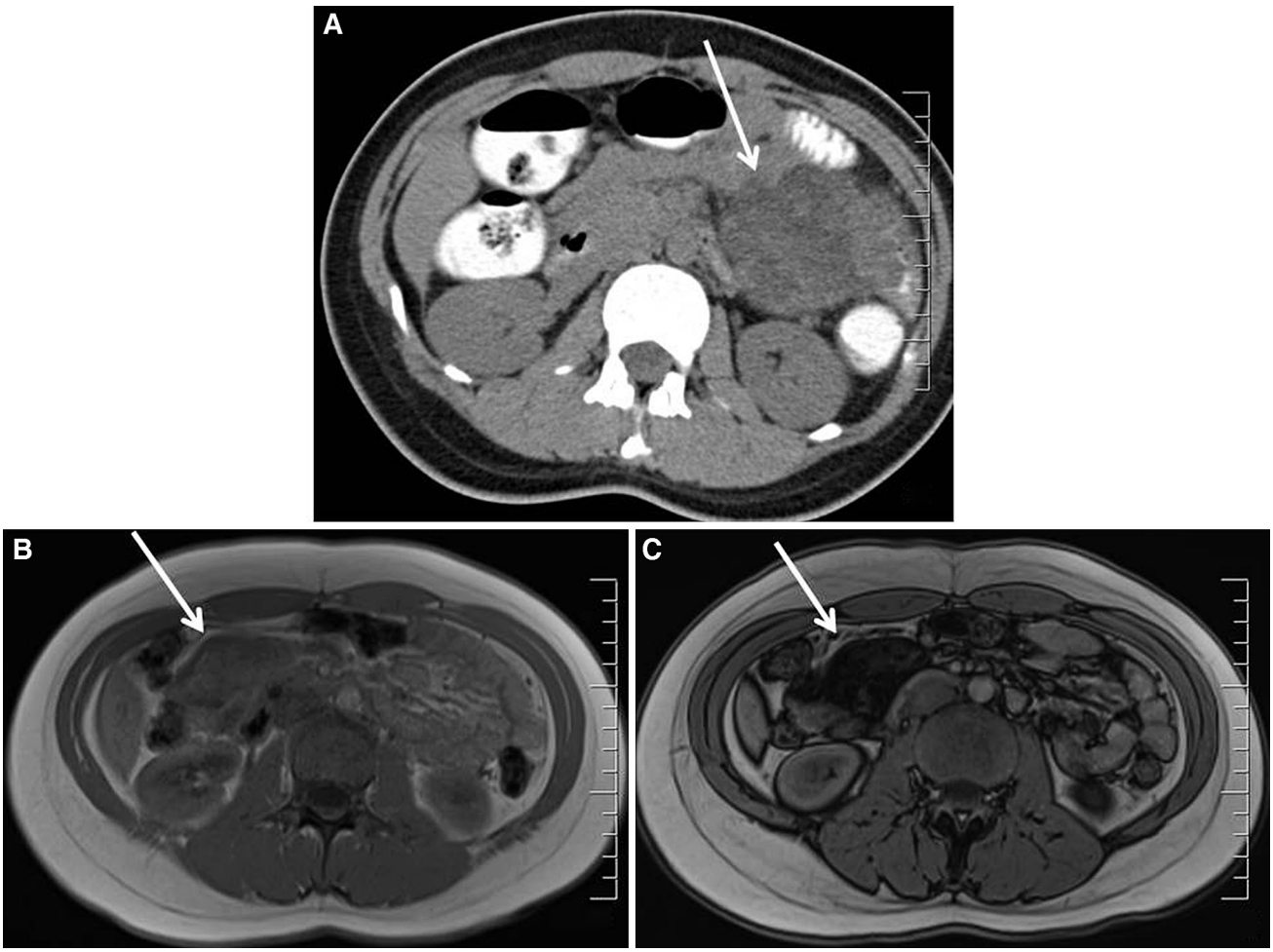

Fig. 10. Mobile mesenteric lymphangioma with internal presence of chyle. **A** Axial contrast-enhanced CT shows left-sided mesenteric cystic mass (*arrow*) in keeping with lymphangioma. **B** Axial in-phase MR image shows a predominantly isointense right-sided round lesion in the mesentery (*arrow*) showing a change of position with respect to the CT. **C** Axial out-of-phase MR image shows dramatic signal loss (*arrow*) relative to the signal intensity on the in-phase image, finding that confirms the presence of water and lipid lesion content.

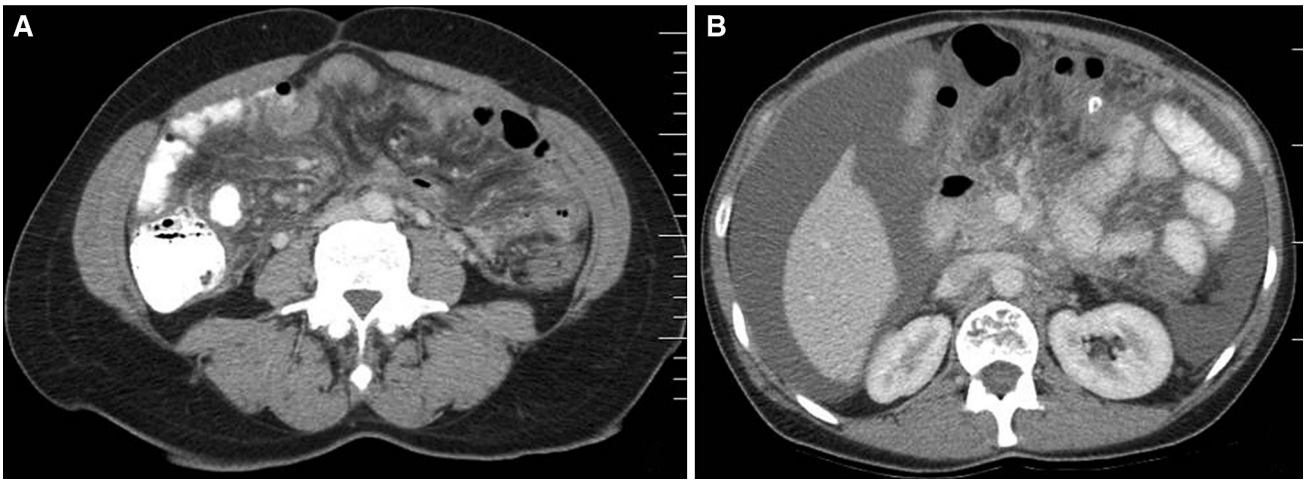

Fig. 11. Lymphangiectasia. **A** 3 years ago. Axial contrast-enhanced CT shows diffuse small bowel thickening with engorgement of the mesentery (villi that contains the dilated lymphatics). **B** 2 months ago. Diffuse ascitis secondary to progression of the generalized lymphangiectasia.

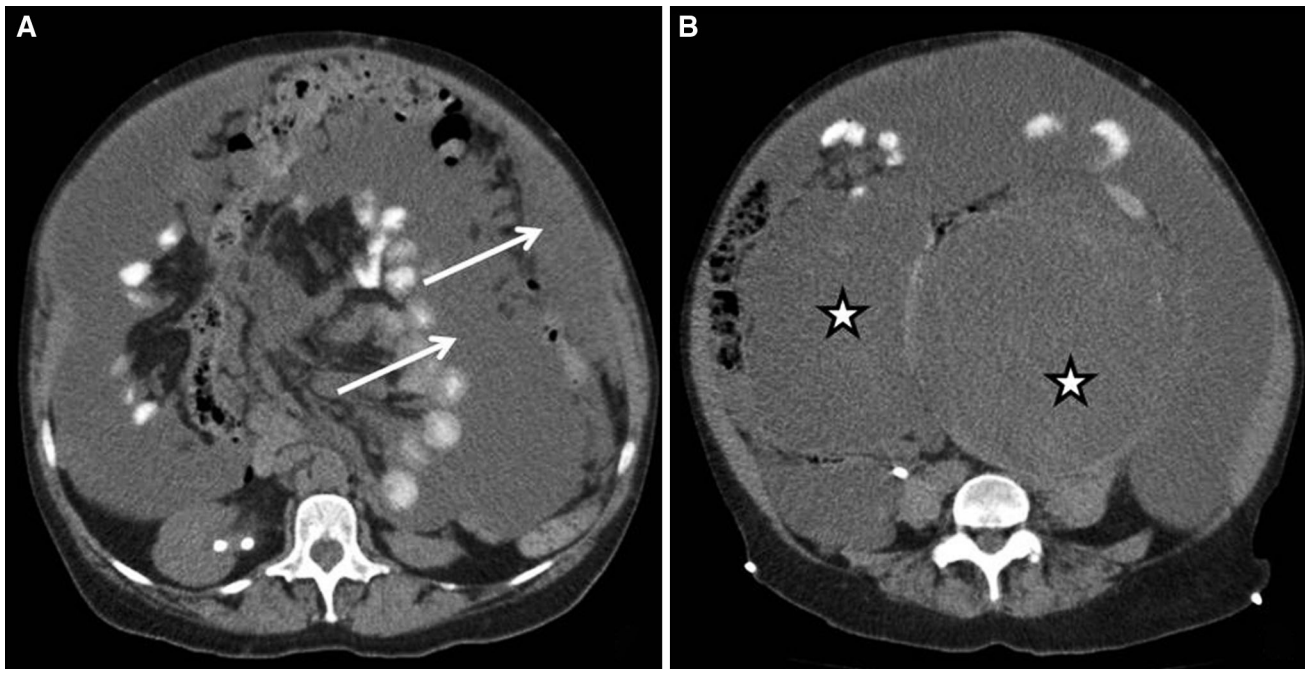

Fig. 12. Pseudomyxoma peritonei. Axial contrast-enhanced CT shows extensive cystic peritoneal disease involving the mesentery (*arrow*) and omentum (*arrow*). Cystic pelvic complex masses are noted (*asterisk*).

demonstrate easily the fatty content within a cyst (Fig. 24).

Infectious

There are infectious processes which may affect the peritoneal cavity and present as cystic lesions, like tuberculosis and hydatid disease.

The abdomen is the most common site of extrapulmonary tuberculosis and abdominal lymphadenopathy is the most common manifestation of abdominal tuberculosis, which appear as cystic lymph nodes with hypoattenuating center and hyperattenuating enhancing rim on CT. There are two types of tuberculous peritonitis, the *wet type* (Fig. 25) with large amount of free or loculated ascites and the *dry type* which associates mesenteric and omental thickening, fibrous adhesions, and caseous nodules.

Intraperitoneal involvement in hydatid disease accounts for 13% of all abdominal hydatidosis [44]. Very rarely primary peritoneal involvement has been described [45]. Peritoneal involvement is thought to be secondary to rupture of hepatic, splenic, or mesenteric cysts. Hydatid cysts are large, unilocular/multilocular, cystic/solid masses. Occasionally, they may have a unilocular morphology with no internal architecture are then difficult to differentiate from mesenteric cysts, or intestinal duplication cysts [46]. US is the most sensitive technique for the detection of internal daughter cysts, floating membranes, and matrix. CT is the best technique to show cyst calcification, infection, and peritoneal seeding (Figs. 26, 27). The most characteristic features with MR is the low-signal intensity rim of the hydatid cyst on T2-weighted images [47] (Fig. 26D) due to abundant collagen content of the pericyst that may aid in making the correct diagnosis when other features are absent.

Cystic with solid component lesions

Cystadenocarcinoma

As detailed above, both cystadenoma and cystadenocarcinoma may arise from the ovary, pancreas, or appendix and may appear cystic. Extensive papillary projections and solid component correlate with increased likelihood of a malignant cystic mass. Cystadenocarcinoma present as cystic masses with enhancing solid/papillary components as well as thick and irregular walls or thick septa with possible ancillary findings like peritoneal implants, ascites, and lymphadenopathy (Figs. 15, 16, 17).

Histologically, features that help distinguish serous cystadenocarcinoma from borderline tumors includes obvious stromal invasion, extensive cellular budding, and confluent cellular growth as well as nuclear atypia (Fig. 17C).

Primary peritoneal serous carcinoma

Primary peritoneal serous carcinoma is an epithelial tumor that arises from the peritoneum [34] and occurs

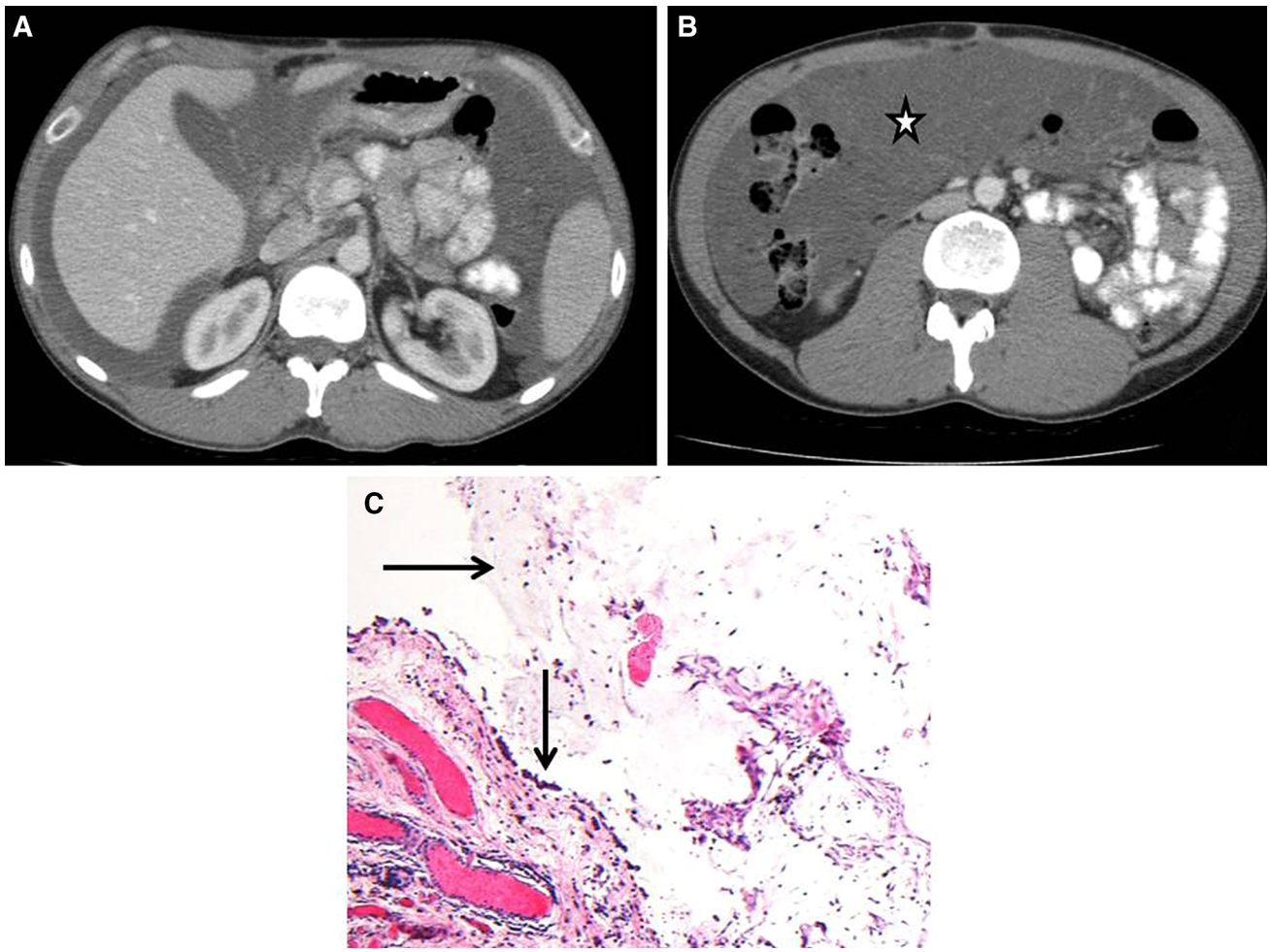

Fig. 13. Mucinous colon carcinoma. Pseudomyxoma peritonei. Axial contrast-enhanced CT (**A**, **B**) shows extensive cystic peritoneal disease involving all the abdomen and pelvis. Note the diffuse omental infiltration (**B**) (*asterisk*) by mucinous tumoral infiltration. C (H&E stain, ×20). Photomicrograph showing pools of mucin (*horizontal arrow*) and adjacent mesothelial lining (*vertical arrow*).

almost always in women (mean age 56–62 years). At histopathologic analysis, it resembles a malignant ovarian surface epithelial stromal tumor. The majority of patients present with ascites and elevation of cancer antigen 125 (CA-125). The most characteristics imaging features are ascites, peritoneal nodules, and thickening and omental nodules and masses [48, 49]. Calcifications within the peritoneal and omental nodules (Fig. 28) represent psammoma bodies histopathologically and occur approximately in 30% of cases. No adnexal masses are detected on the majority of patients of primary peritoneal serous carcinoma.

Malignant cystic mesothelioma

Most malignant peritoneal mesotheliomas occur in older men during fifth and sixth decades and are associated with asbestos exposure. Malignant mesothelioma tend to spread in sheets of tissue over the parietal and visceral peritoneal surfaces and to become confluent, encasing abdominal organs [50]. There are a couple of CT appearances of malignant peritoneal mesothelioma, the "dry" type consisting of peritoneum-based masses and the "wet" type (Fig. 29) consisting of ascites, irregular, or nodular peritoneal thickening and an omental mass. Differential diagnosis of the "wet" type malignant mesothelioma includes peritoneal carcinomatosis, serous surface papillary carcinoma, lymphomatosis, and tuberculosis on the basis on the CT findings. One of the CT features that can help in the diagnosis is that the amount of ascites is disproportionately small in relation to the degree of tumor dissemination in malignant mesothelioma when comparing with peritoneal carcinomatosis, although malignant mesothelioma remains as a diagnosis of exclusion.

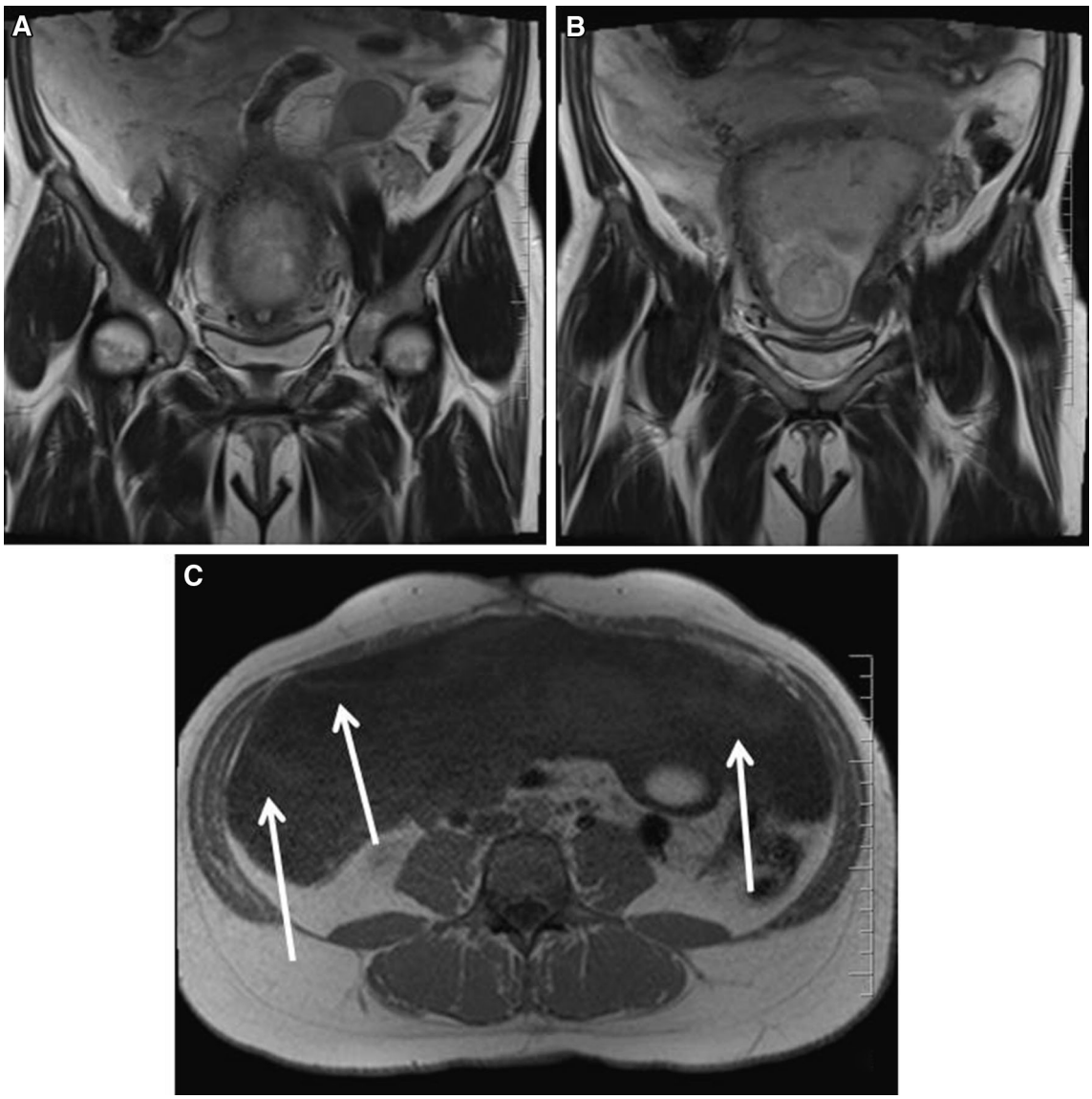

Fig. 14. Pseudomyxoma peritonei. Pregnant patient. **A**, **B** Coronal T2-weighted MR images. **C** Axial T1-weighted MR image. There is evidence of extensive cystic peritoneal disease in a pregnant patient, predominantly hyperintense on T2-WI and hypointense on T1-WI. There are subtle areas of T1 hyperintense signal, (*arrows*) probably related to thicker mucin.

Sex cord gonadal stromal tumors: granulosa cell tumor

Granulosa cell tumor is a neoplasm composed of a pure or at least 10% population of granulosa cells often in a fibrothecomatous background. There are two major subtypes, adult type which occurs in women over 40 representing 95% of all granulosa cell tumors and juvenile type. The tumor secretes estrogen so therefore this tumor should be considered when an endometrial lesion is seen in association with heterogeneous solid adnexal mass. Patients commonly present with metrorrhagia or postmenopausal bleeding in the adult type and isosexual precocious in pediatric population.

On US granulosa, cell tumor is usually large multiloculated cystic masses with thin or thick internal septations, and solid component, although papillary projections and calcifications, common in epithelial ovarian tumors are not usually seen. Endometrial thickening due to hormone secretion are seen in 50% of patients and endometrial adenocarcinoma in 10% [51]. On CT solid enhancing mass with variable cystic or hemorrhagic/degenerating areas of low attenuation is usually seen associated with enlarged uterus with endometrial thickening. On MR high T1 content of the cysts is typical, reflecting intralesional hemorrhage. Metastases may occur through direct extension and intraperito-

Fig. 15. CT appearance of mucinous cystadenocarcinoma of the ovary. Axial contrast-enhanced CT shows a multiloculated predominantly cystic mass in the pelvis with numerous enhancing internal septa (*arrows*) in pelvis.

neal seeding, or hematogeneously to the lungs, liver, and brain. Rarely, extra ovarian primary granulosa cell tumor may be seen as cystic masses in the abdomen (Fig. 30).

Cystic mesenchymal tumors

Gastrointestinal stromal tumors (GISTs) are the most common mesenchymal neoplasms of the gastrointestinal tract and may also occur primarily in the omentum, mesentery, and retroperitoneum [52]. GISTs have tendency to exophytic growth and the histologic classification is based on the predominant cell type, either spindle or epithelioid cell [53, 54]. They are mostly seen in older patients except when associated with tumor syndromes like neurofibromatosis type 1 and patients with Carney triad when they may present earlier and are often multiple. Many tumors are incidentally identified on imaging for other indications, and some of them on the other hand are aggressive and present with metastases or symptoms relating to local disease [52]. On imaging these are often solid, with variable degrees of necrosis within the mass, depending on tumor size. Many GISTs achieve enormous size before diagnosis and demonstrate considerable cystic change and at times may appear predominantly cystic [55] (Fig. 31). Intratumoral hemorrhage has also been described (Fig. 32).

Secondary cystic peritoneal lesions as potential mimickers

There are many intrabdominal processes which may mimic cystic masses within the peritoneal cavity. These include various fluid collections such as abscess, seroma, biloma, urinoma, lymphocele, urachal cyst, or aneurysm of mesenteric artery branches.

- Urinomas are encapsulated collections of chronically extravasated urine secondary to penetrating or iatrogenic injury. They are usually located along the course of the urinary tract, in the perirenal space, retroperitoneum, or pelvis. On US, they are simple or complex fluid collections and on CT are hypoattenuating water density fluid collections (Fig. 33) with demonstration of contrast leakage within the fluid collection on delayed post-contrast imaging.
- Lymphoceles usually occur after pelvic lymphadenectomy, hysterectomy, prostatectomy, or renal transplant surgery and are fluid-filled cysts without an epithelial lining abutting surgical clips after surgery [43]. On US, they are anechoic or hypoechoic masses with acoustic enhancement, and may have dependent debris and septations. On CT, calcification along the wall may be seen although is uncommon. On MR, lymphoceles show low intensity on T1-weighted images and high signal intensity on T2-weighted images (Fig. 34).
- Bilomas are collections of fluid within the liver or close to the biliary tree which may develop iatrogenically, secondary to a trauma or spontaneously due to a bile duct rupture. The size of the collection depends on the difference between leakage rate and reabsorption rate of bile by the peritoneum/surroundings. On imaging they are usually unilocular, have a thin capsule and are of low attenuation.
- Urachal cyst is one of the spectrum of congenital urachal remnant abnormalities [56]. A urachal cyst develops if the urachus closes at both the umbilicus and the bladder but remains patent between two endpoints. Urachal cysts become symptomatic when they enlarge or are complicated by infection or bleeding. An uncomplicated urachal cyst appears as a collection of simple fluid localized in the midline of the anterior abdominal wall (Fig. 35) [57, 58], between the umbilicus and the pubis and often contiguous with the bladder dome.

Other specific characteristics of certain collections may also facilitate diagnosis like gas within an abscess (Fig. 36) or an infected collection, or the presence of flow/contrast material within splanchnic aneurysms and pseudoaneurysms (Fig. 37). On MR high T1 signal intensity within a fluid collection on fat-suppressed images is suggestive of blood products, implying possibility of a hematoma or seroma.

These collections need to be identified and differentiated from primary cystic masses as some of these collections (abscess, urinoma, biloma, or splanchnic aneurysms) may require urgent intervention. At times surgical excision or needle aspiration of the fluid may be needed to make a definitive diagnosis.

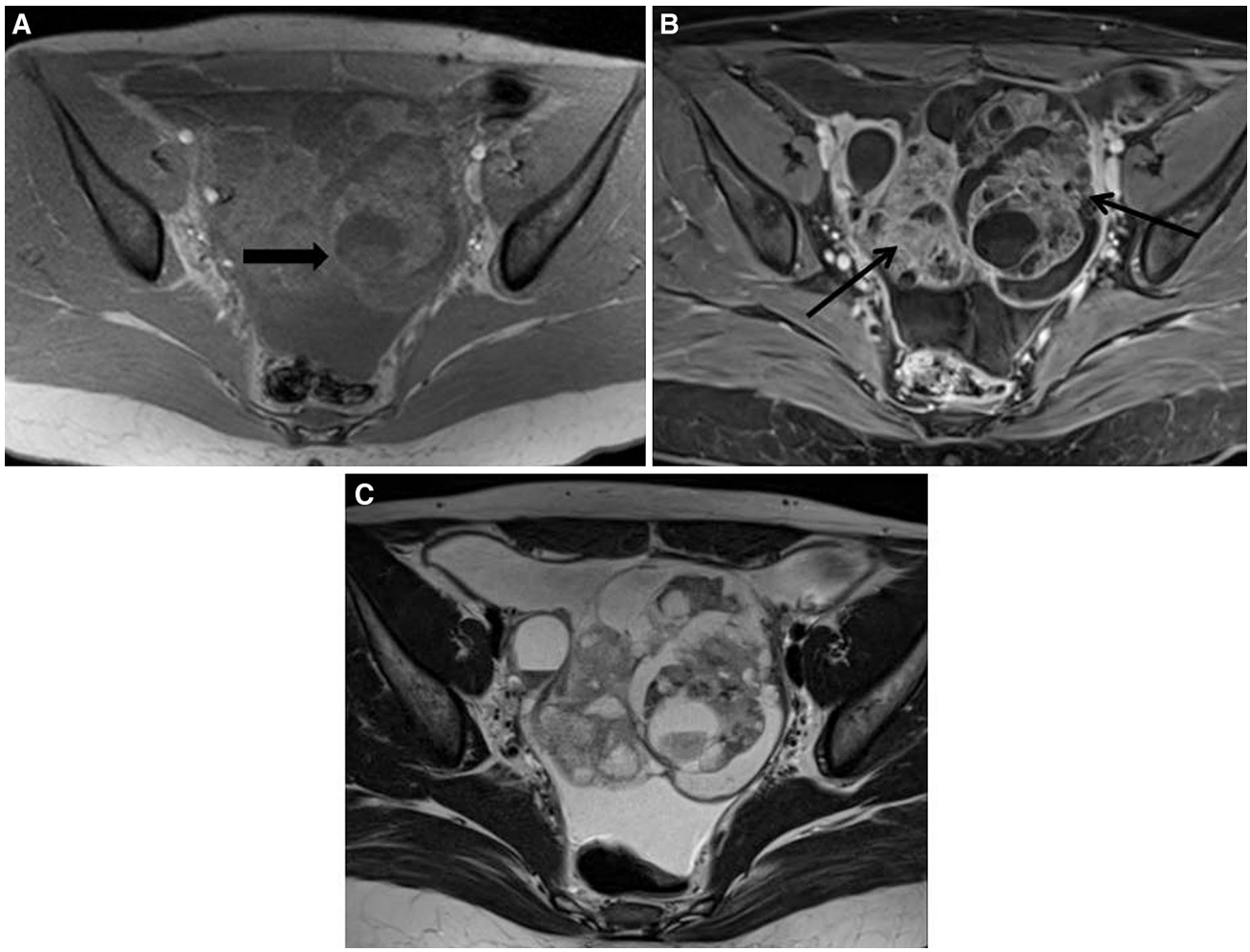

Fig. 16. MRI appearance of mucinous cystadenocarcinoma of the ovary. **A** Axial T1-weighted MR image pre-contrast. **B** Axial T1-weighted MR image after contrast. **C** Axial T2-weighted MR image. There is evidence of a large complex cystic predominantly T2 hyperintense mass originating from the left ovary (not shown) with some solid areas with avid enhancement after intravenous contrast (*arrows*). The lesion contains loculated small cystic areas, some of them demonstrating fluid–fluid level (*thick arrow* in **A**) with T1 hyperintense component probably related to proteinaceous, mucinous, or hemorrhagic contents.

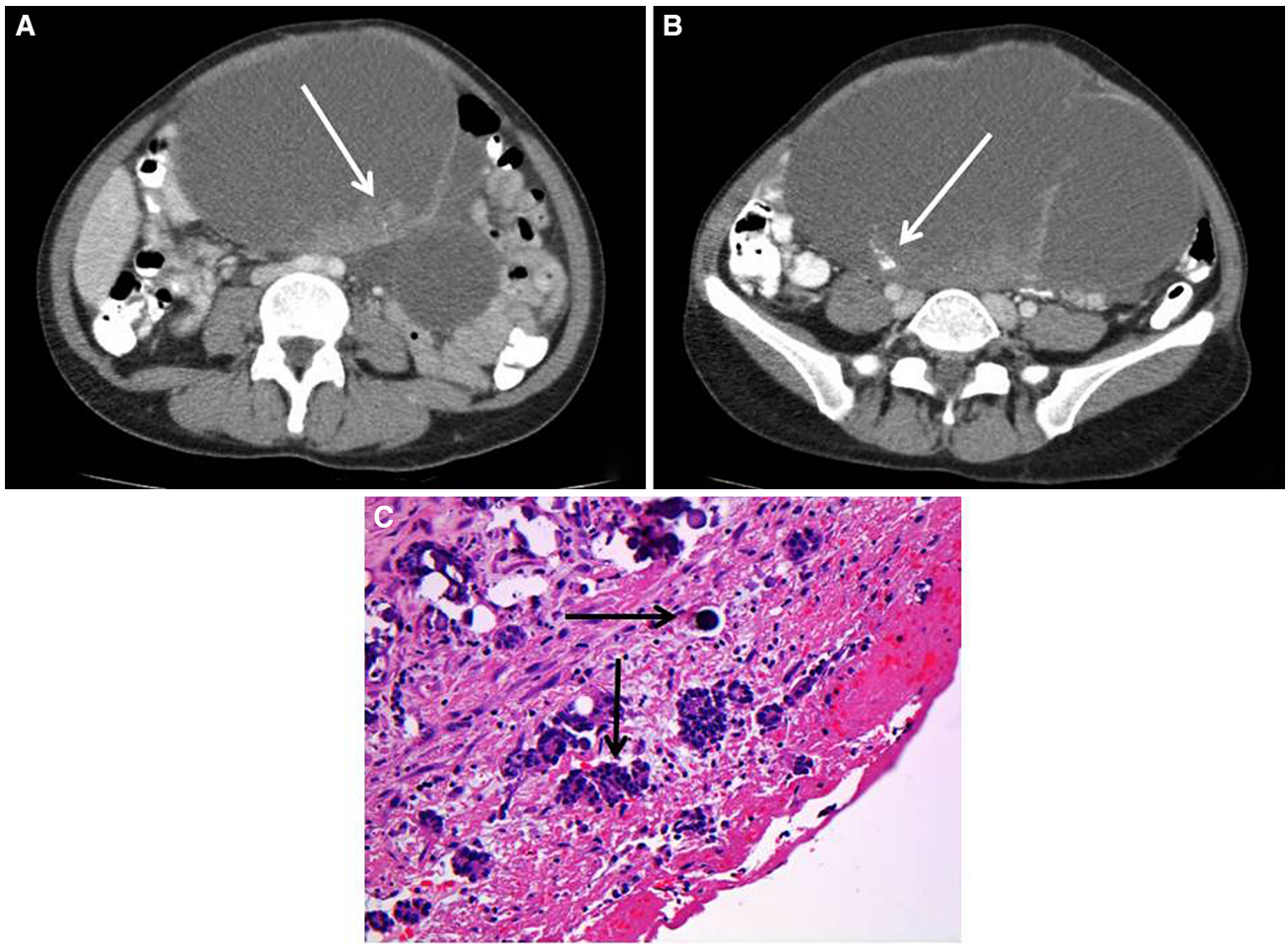

Fig. 17. Serous cystadenocarcinoma of the ovary. Axial contrast-enhanced CT shows a large multiloculated cystic mass arising from the pelvis. Note there is enhancing soft tissue within the mass (**A**) (*arrow*) and calcifications within the mass related to psammomatous calcifications (**B**) (*arrow*). **C** (H&E stain, ×40): low grade serous carcinoma. Psammomatous calcification (*horizontal arrow*) and tumor cells within cyst wall (*vertical arrow*).

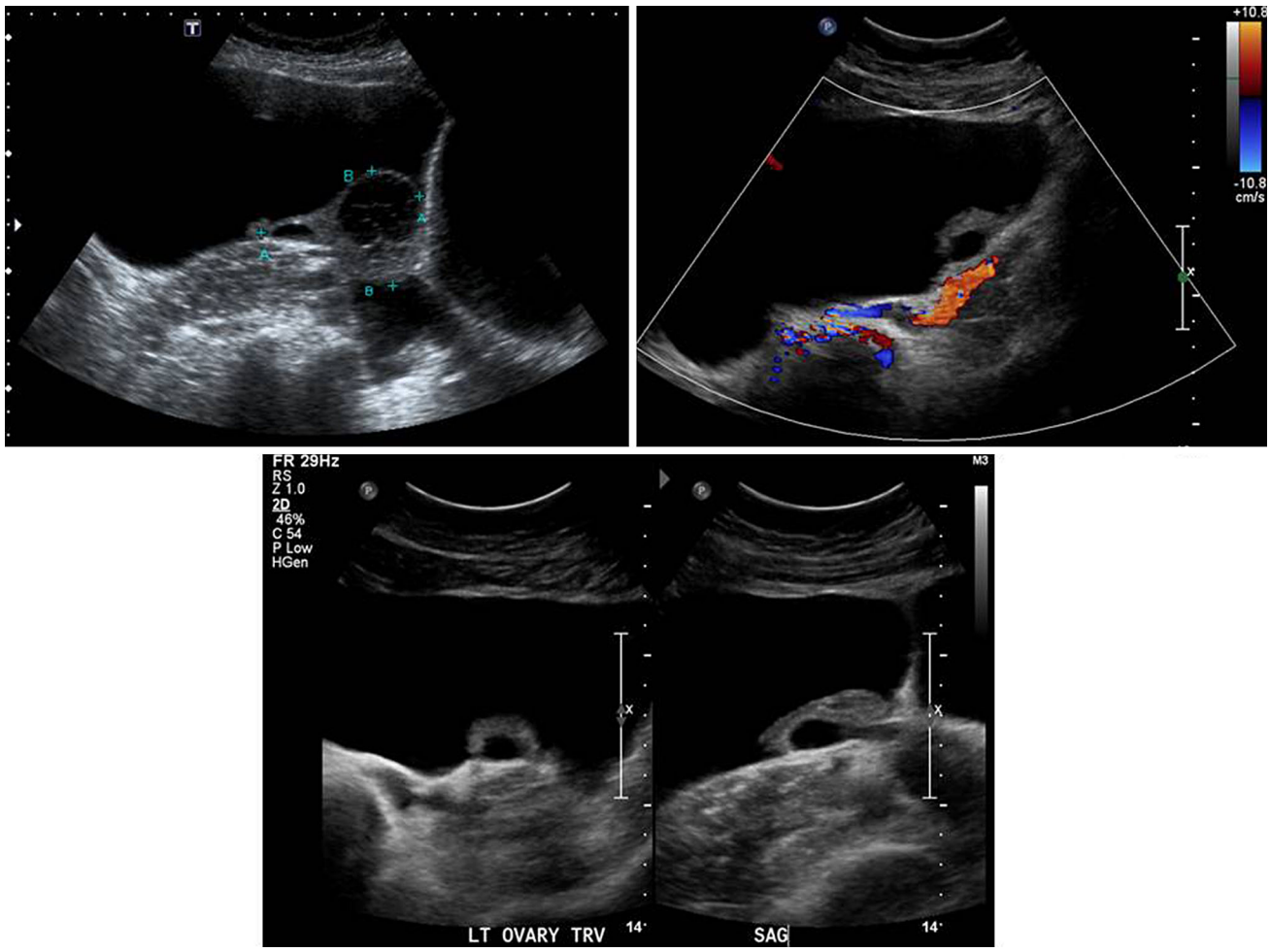

Fig. 18. Peritoneal inclusion cyst. **A**–**C** Pelvic US showing a cystic mass encasing/surrounding left ovary.

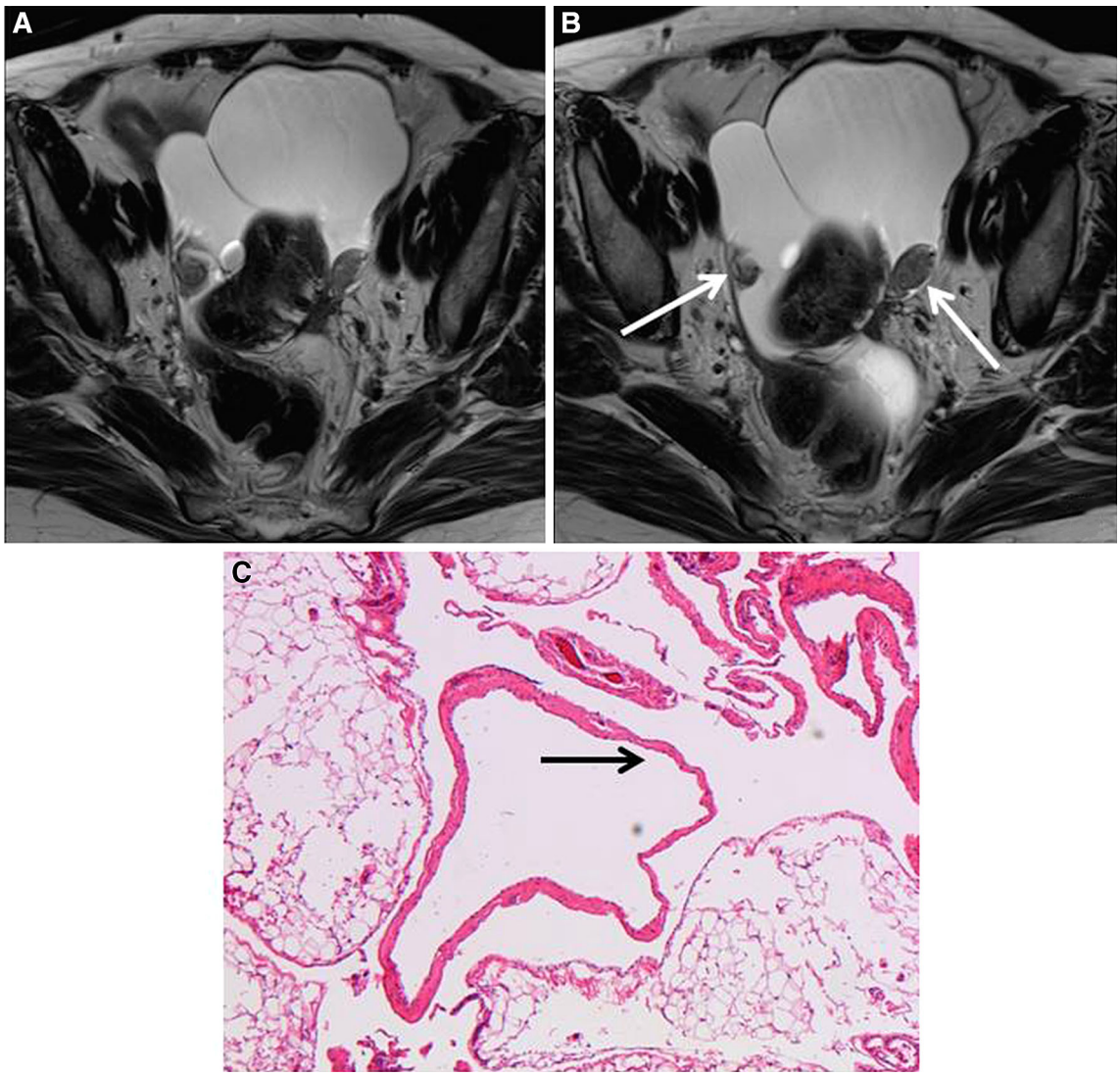

Fig. 19. Peritoneal inclusion cyst. **A**, **B** Axial T2-weighted MR images show homogeneous high signal intensity mildly complex fluid collection in pelvis. Note that both ovaries appear completely surrounded by the cystic mass bilaterally (*arrows*). **C** (H&E stain, ×10): Cyst lined by flattened mesothelial lining (*arrow*) with adjacent omental fat.

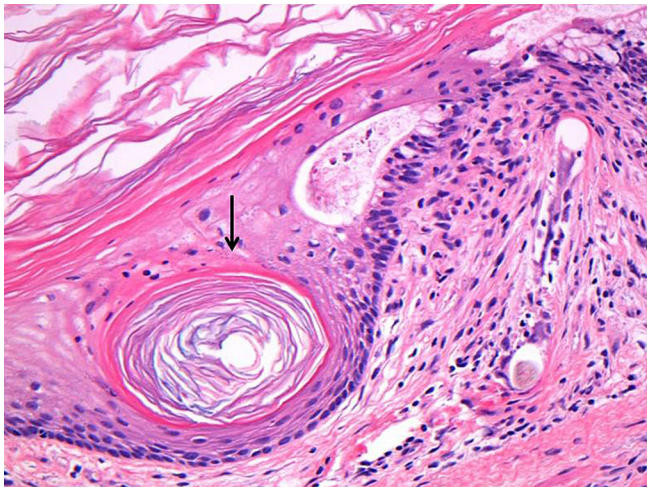

Fig. 20. Cystic teratoma (H&E stain, ×40): part of cyst wall showing squamous epithelium with adnexal structures, hair shafts (*arrow*).

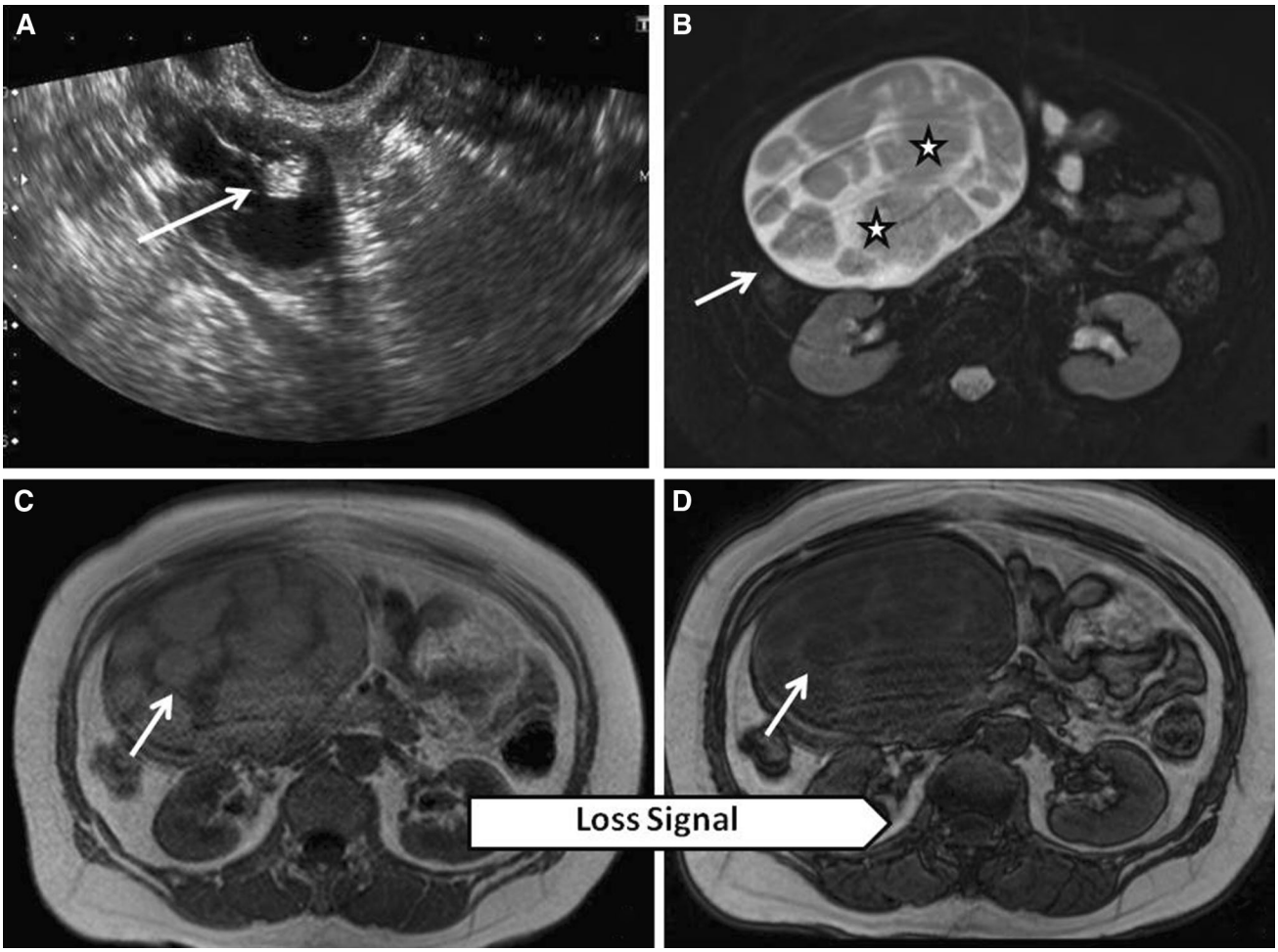

Fig. 21. Cystic teratoma. **A** Transverse sonogram shows complex cystic and solid mass in the right ovary with an echogenic solid appearance peripheral nodule related to fatty content (*arrow*). **B** Axial T2-weighted MR image shows in the right midabdomen arising from the ovary (not shown) a complex hyperintense cystic mass (*arrow*) with large round intralesional hypointense components (*asterisks*). Axial in-phase T1 GRE (**C**) and out-of-phase T1 GRE (**D**) MR images show signal loss on the out-of-phase compared to the in-phase sequences suggesting microscopic fat (*arrows*).

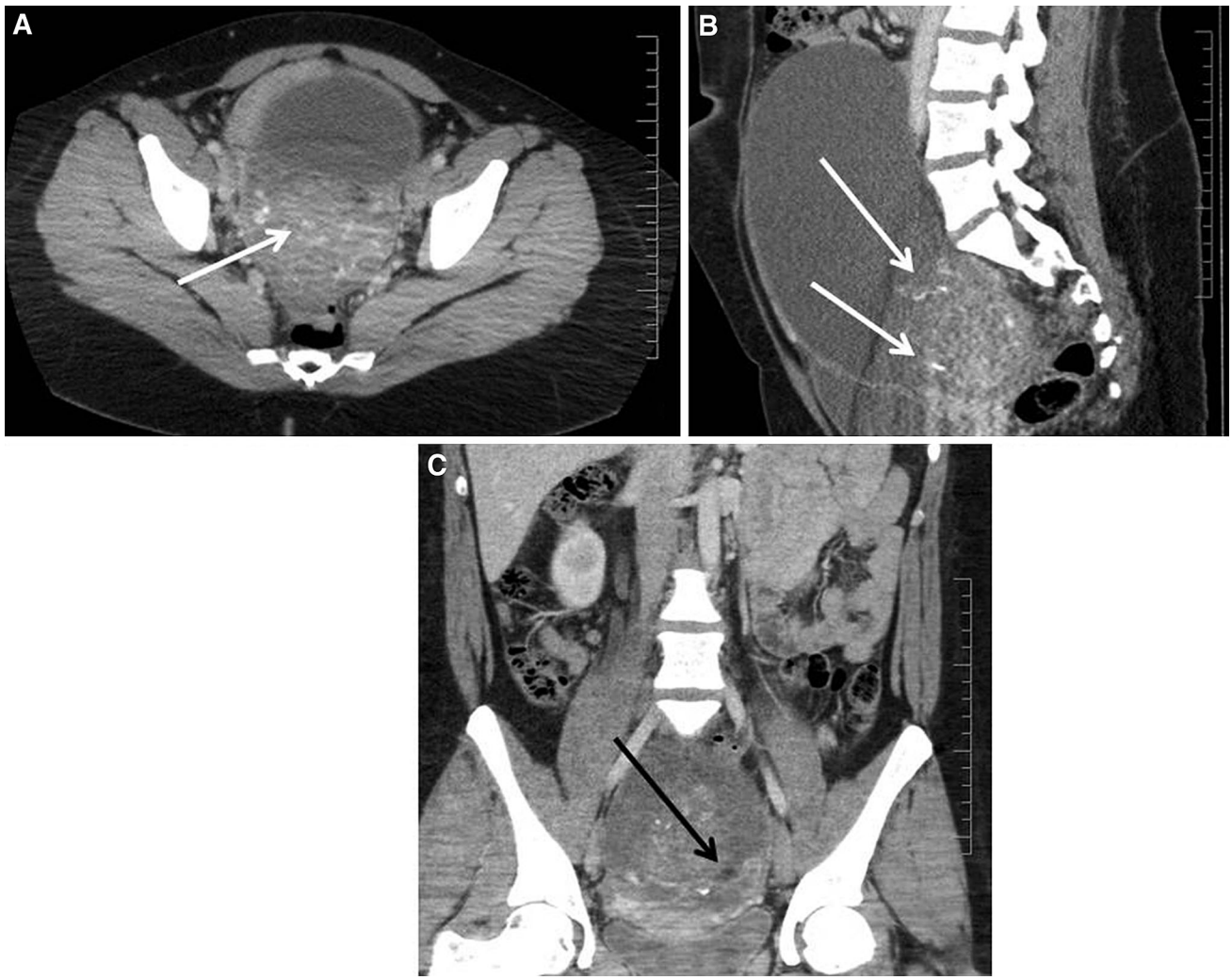

Fig. 22. Immature teratoma. **A** Axial, **B** sagittal, and **C** coronal contrast-enhanced CT shows a large complex cystic and solid mass occupying the lower abdomen containing low-attenuation tiny foci related to fat (*black arrow*) and scattered punctate calcifications (*white arrows*).

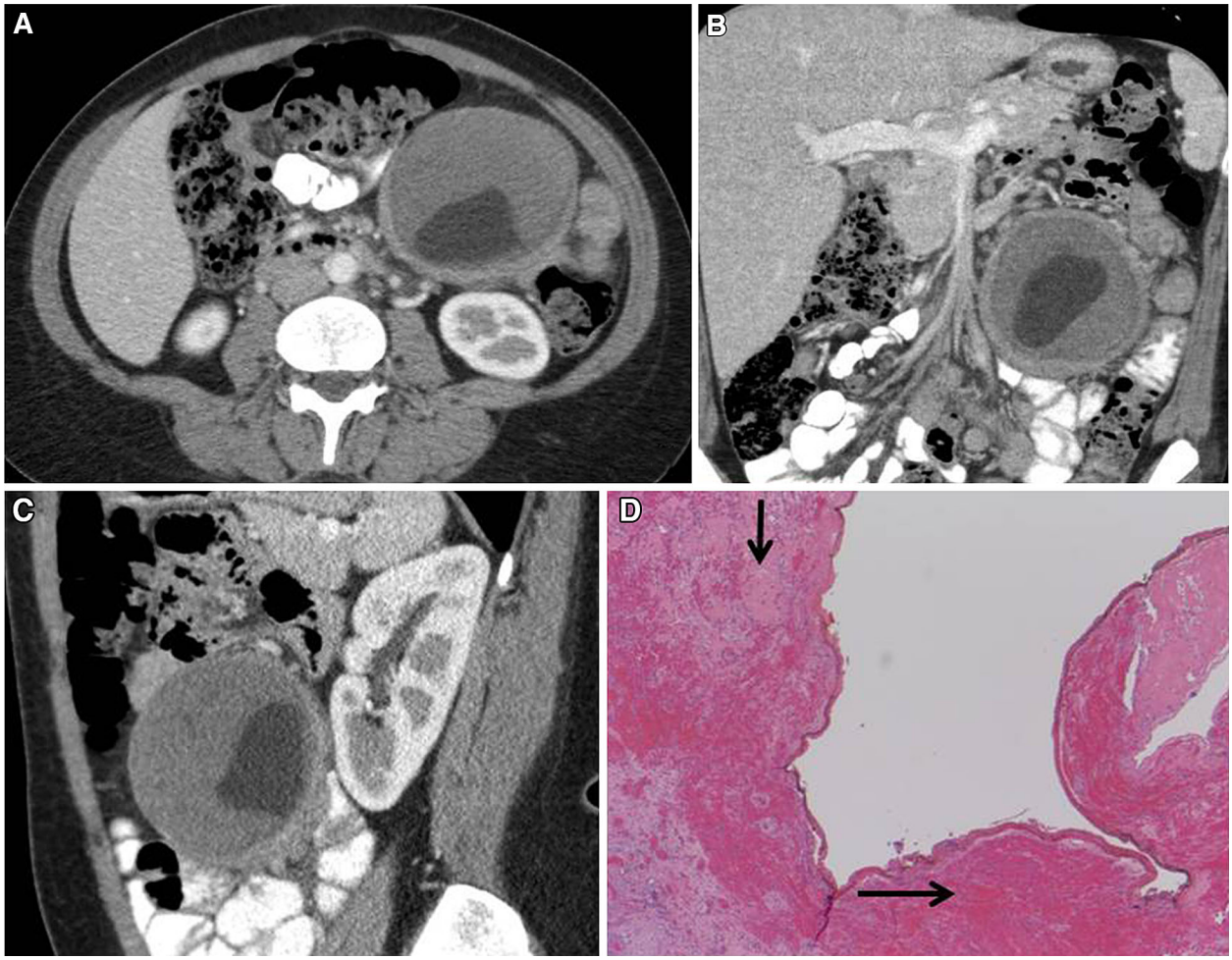

Fig. 23. Traumatic peritoneal pseudocyst. **A** Axial, **B** coronal, and **C** sagittal contrast-enhanced CT image show a thick-walled cystic complex mass in the left midabdomen containing a fat loculated area within. **D** Example of a pseudocyst (H&E stain, ×5): cystic space with no lining epithelium, showing areas of hyalinization (*vertical arrow*) and hemorrhage (*horizontal arrow*).

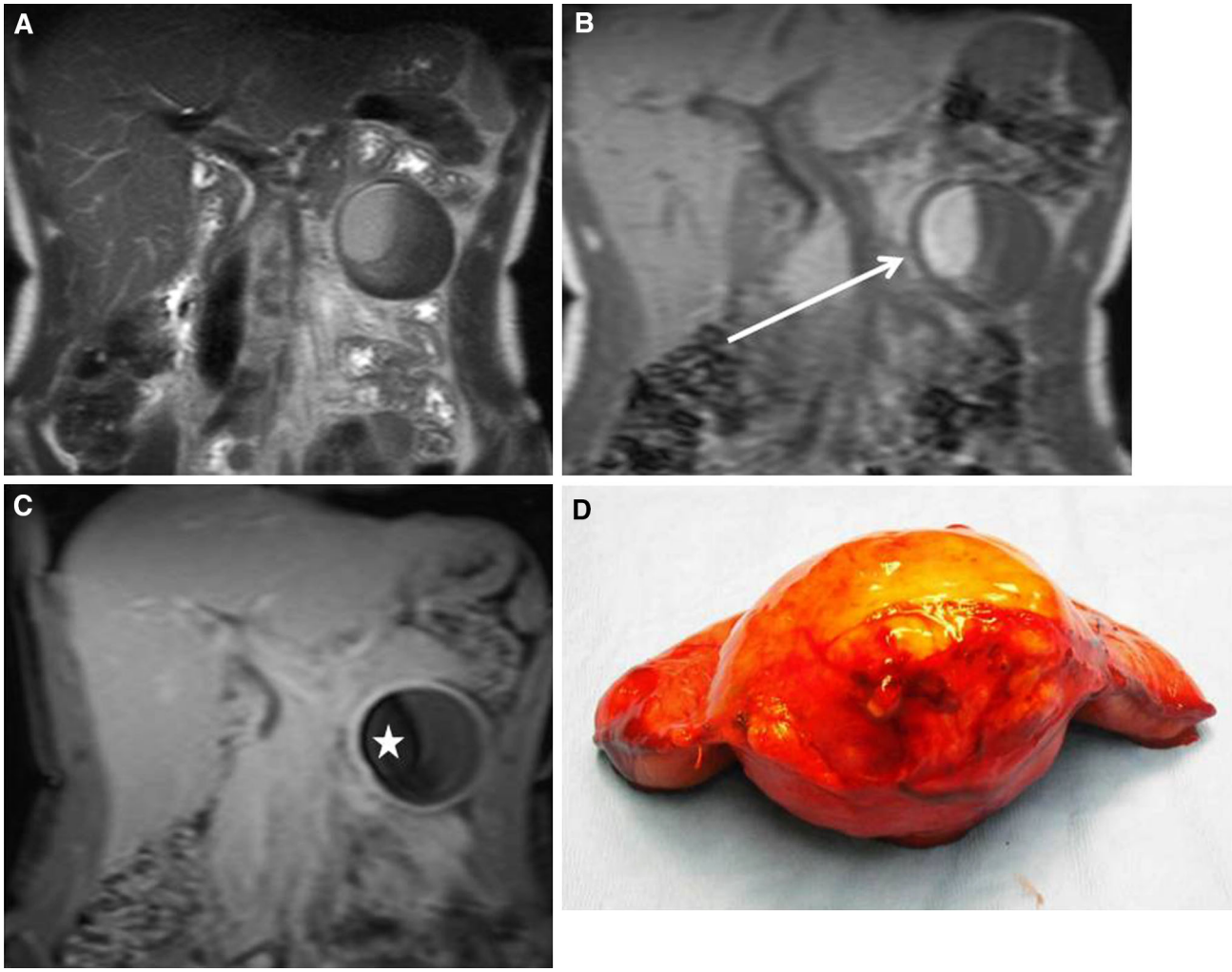

Fig. 24. Traumatic peritoneal pseudocyst. **A** Coronal T2-weighted MR image shows a complex cystic mass in left upper quadrant. **B** Coronal T1-weighted MR image of the mass shows high signal in a component of the cyst (*arrow*). **C** Coronal fat-saturated post-contrast T1-weighted image of the mass shows signal drop in that portion of the cyst content (*asterisk*), confirming it to be fat and showing as well cystic wall enhancement. **D** Gross specimen demonstrating the traumatic peritoneal pseudocyst.

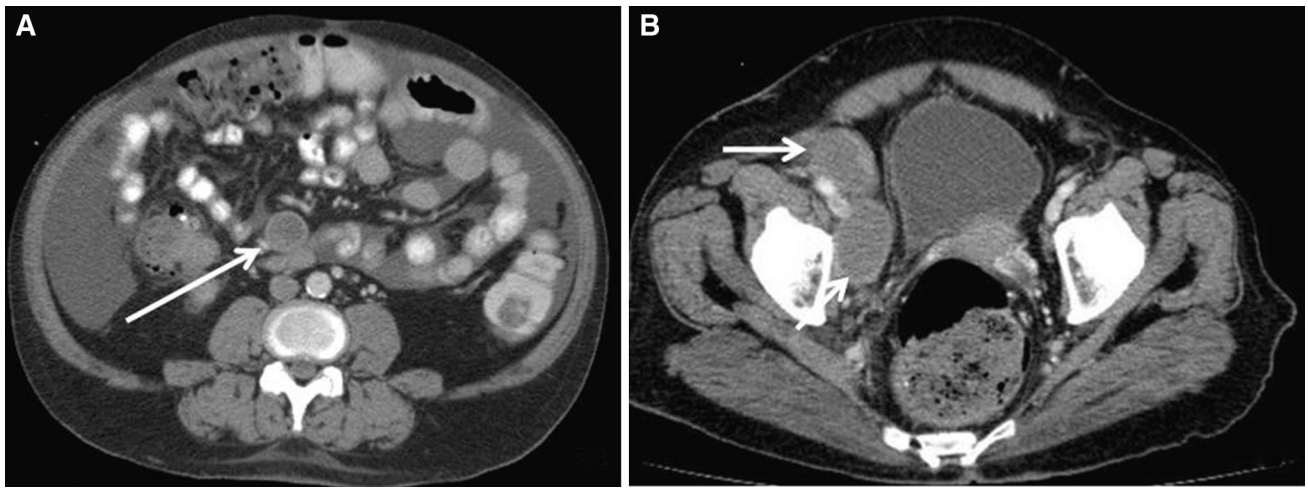

Fig. 25. Abdominal tuberculosis (TB). Wet type. **A**, **B** Axial contrast-enhanced CT image shows enlarged lymphadenoapthy within the retroperitoneum (**A**) (*arrow*) and pelvis (**B**) (*arrow*). Characteristically, these lymphadenopathy have hypodense center (characteristic of caseous necrosis) and peripheral rim enhancement, findings highly suspicious for TBC. Note moderate amount of ascitis.

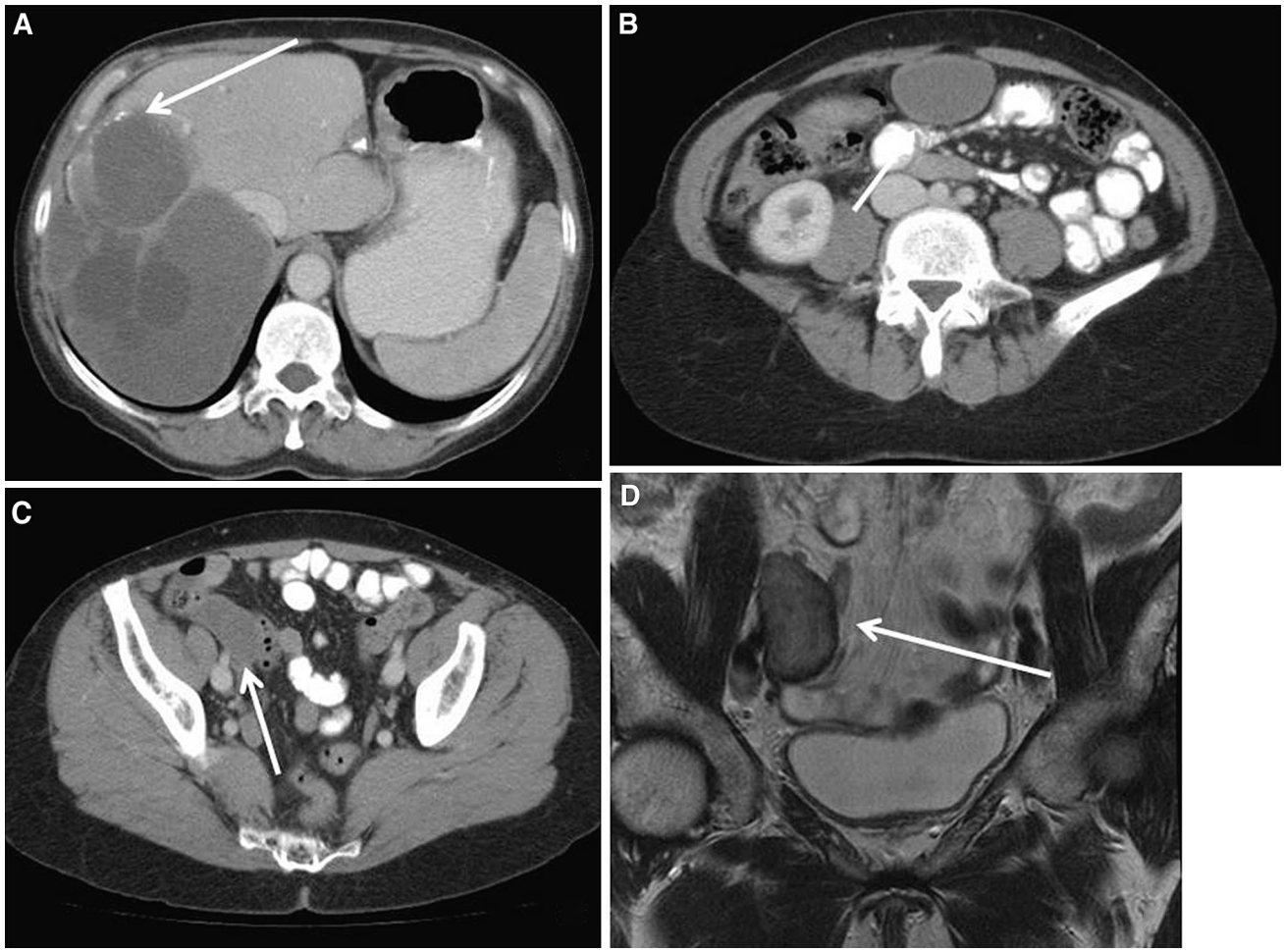

Fig. 26. Hydatid disease. **A** Contrast-enhanced CT axial image shows hepatic hydatic cysts some of which are peripherally calcified (*arrow*). **B**, **C** Contrast-enhanced CT shows several fluid attenuation round lesions within the abdomen and the pelvis in keeping with multiple peritoneal hydatid cysts (*arrows*). **D** Coronal T2-weighted image shows an oval shaped moderately T2 hyperintense cystic lesion medial to the right external iliac vessels (*arrow*) with a characteristic low-signal intensity rim due to abundant collagen content of the pericyst.

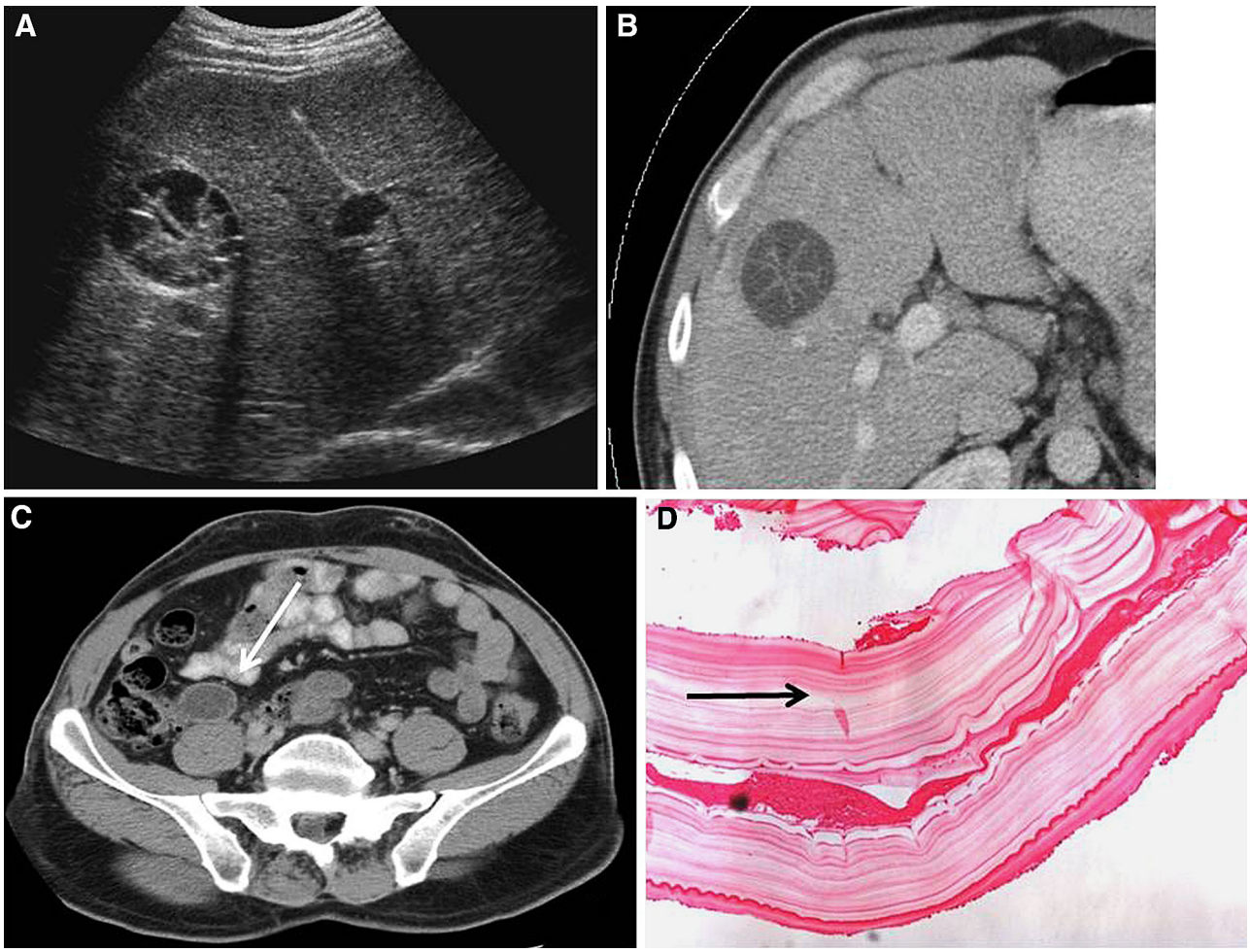

Fig. 27. Hydatid disease. **A** US and **B** CT of the liver shows a complex septated hydatid liver cyst. **C** Contrast-enhanced CT axial image shows a fluid attenuation lesion anterior to the right psoas muscle in keeping a peritoneal hydatid cyst (*arrow*). **D** (H&E stain, ×20): acellular laminated membrane of hydatid cyst (*arrow*).

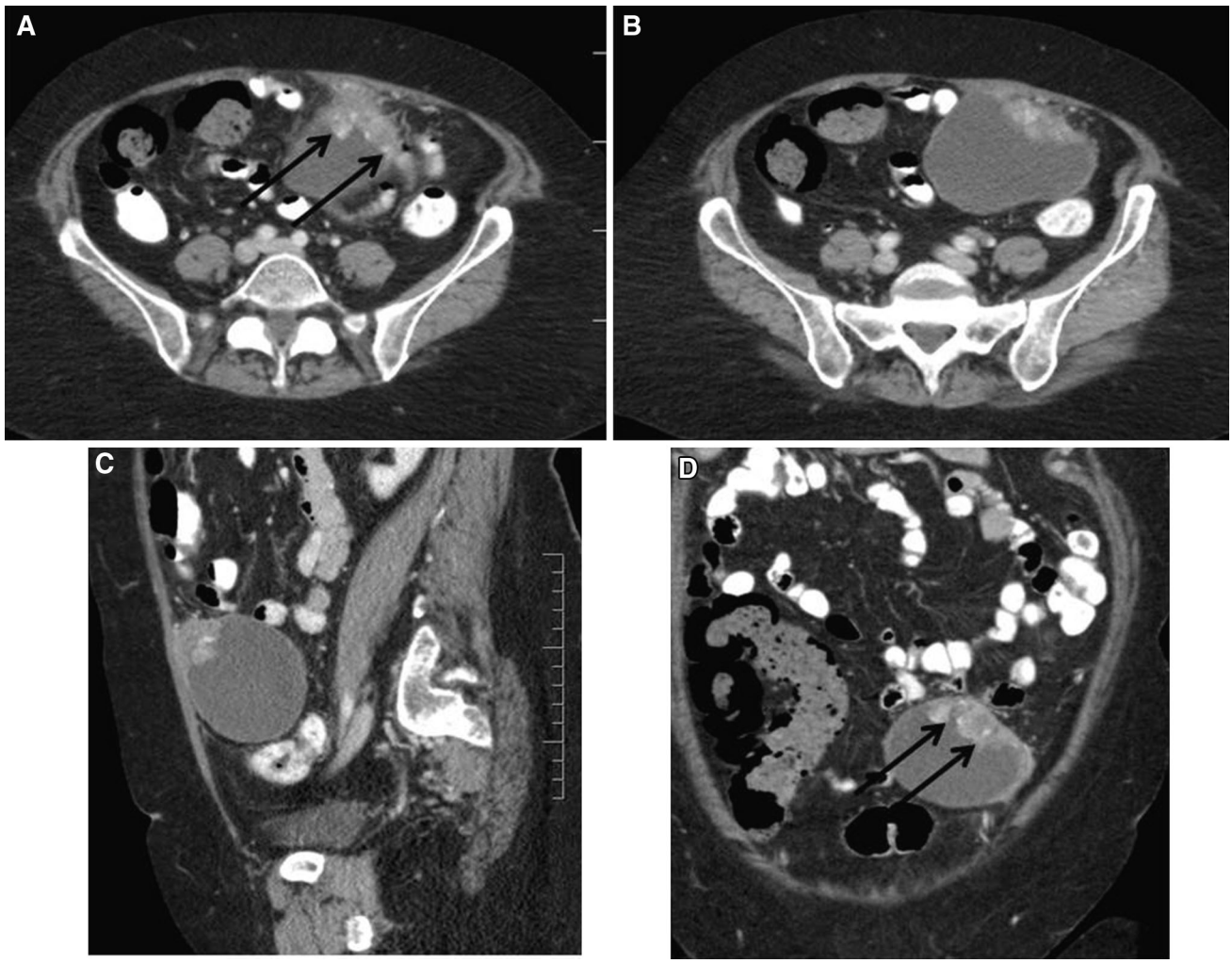

Fig. 28. Primary peritoneal high grade serous carcinoma. **A**, **B** Axial, **C** sagittal, **D** coronal contrast-enhanced CT shows peritoneal nodular thickening arising from left lower quadrant with adjacent loculated ascitis, given the appearance of a cystic mass arising from the peritoneum. Note the presence of tiny calcifications within the nodular thickening related to psammomatous calcifications (*arrows*).

Fig. 29. Malignant mesothelioma. Axial CT image shows diffuse cystic peritoneal disease as well as omental tumoral infiltration (*arrows*).

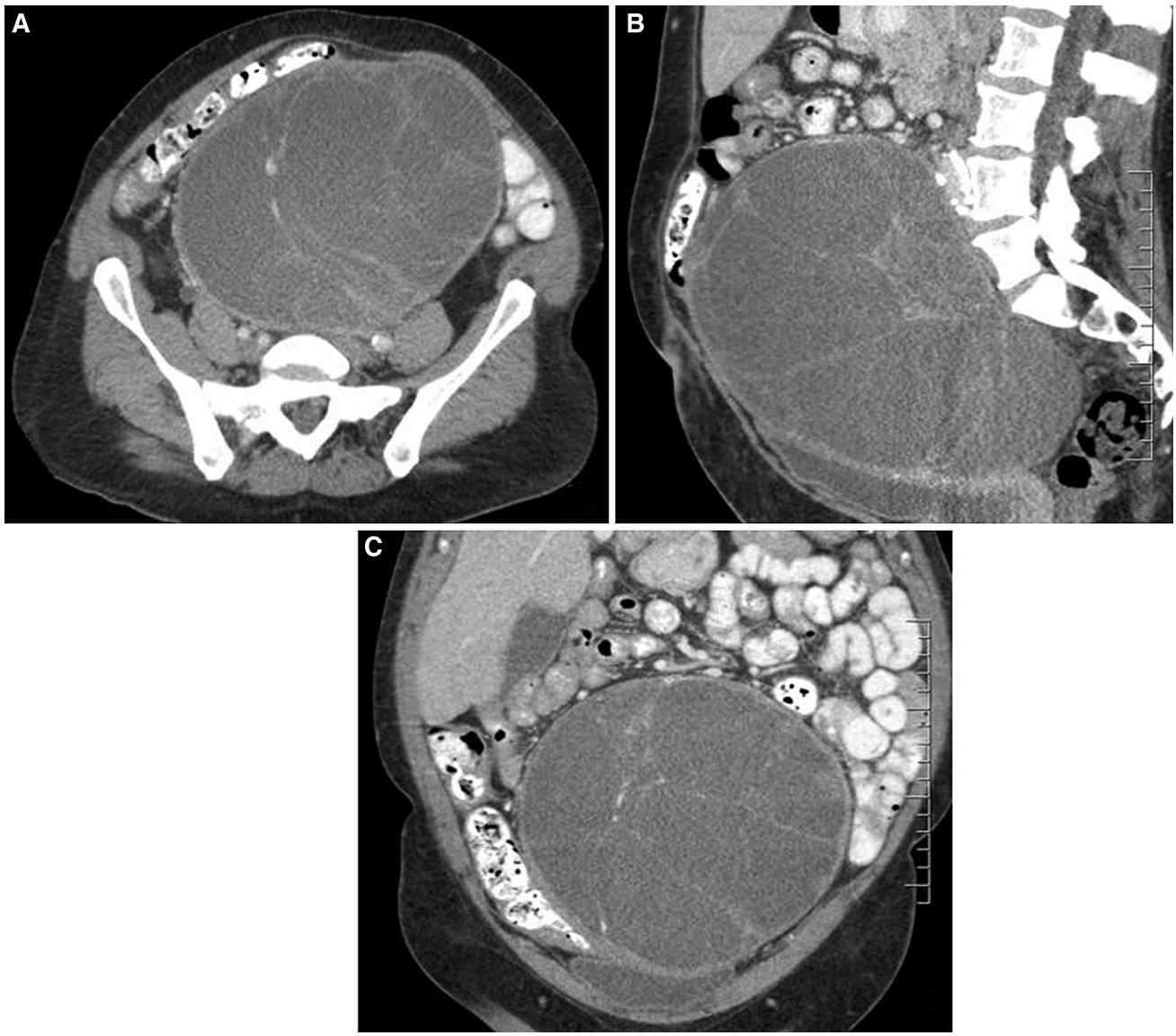

Fig. 30. Retroperitoneal granulosa cell tumor. **A** Axial, **B** sagittal, **C** Coronal contrast-enhanced CT images shows a large multicystic mass with internal septations in the pelvis. Ovaries were demonstrated to be normal.

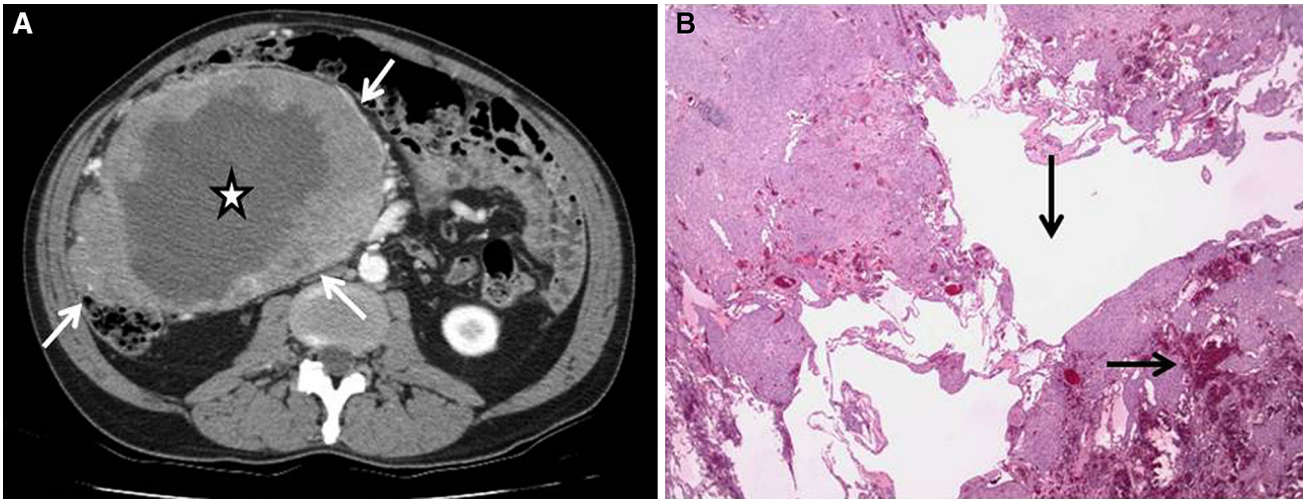

Fig. 31. Gastrointestinal stromal tumor (GIST) with central necrosis. **A** Axial contrast-enhanced CT shows a large predominantly necrotic mass in the proximal small bowel mesentery. The periphery of the lesion is solid in appearance (*arrows*), with evidence of enhancement after intravenous contrast. The center of the mass is hypoattenuated, with cystic appearance secondary to tumoral necrosis (*asterisk*). **B** (H&E stain, ×5): spindle cell tumor with areas of hemorrhage (*horizontal arrow*) and central area of cystic degeneration (*vertical arrow*).

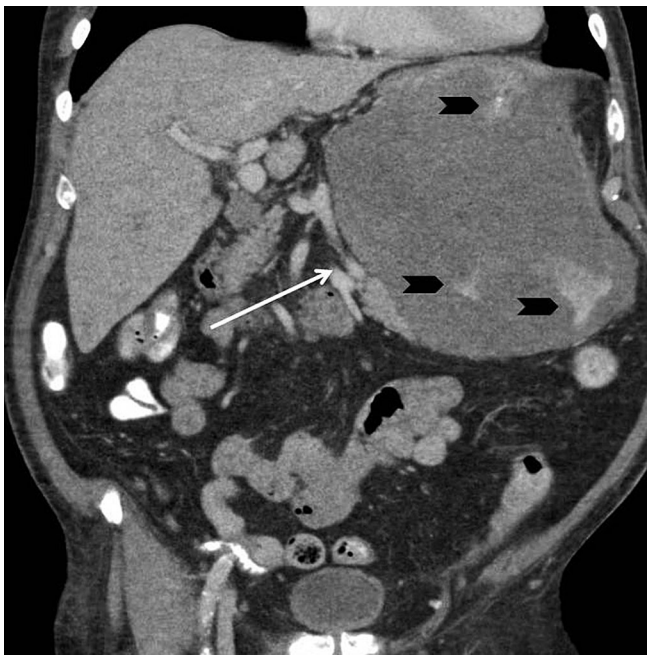

Fig. 32. Hemorrhage within an exophytic GIST, appearing as a cystic mass. Coronal contrast-enhanced CT image shows a cystic mass (*arrow*), with linear high-attenuation areas within due to intravenous contrast extravasation in keeping with ongoing active bleeding (*small arrowheads*).

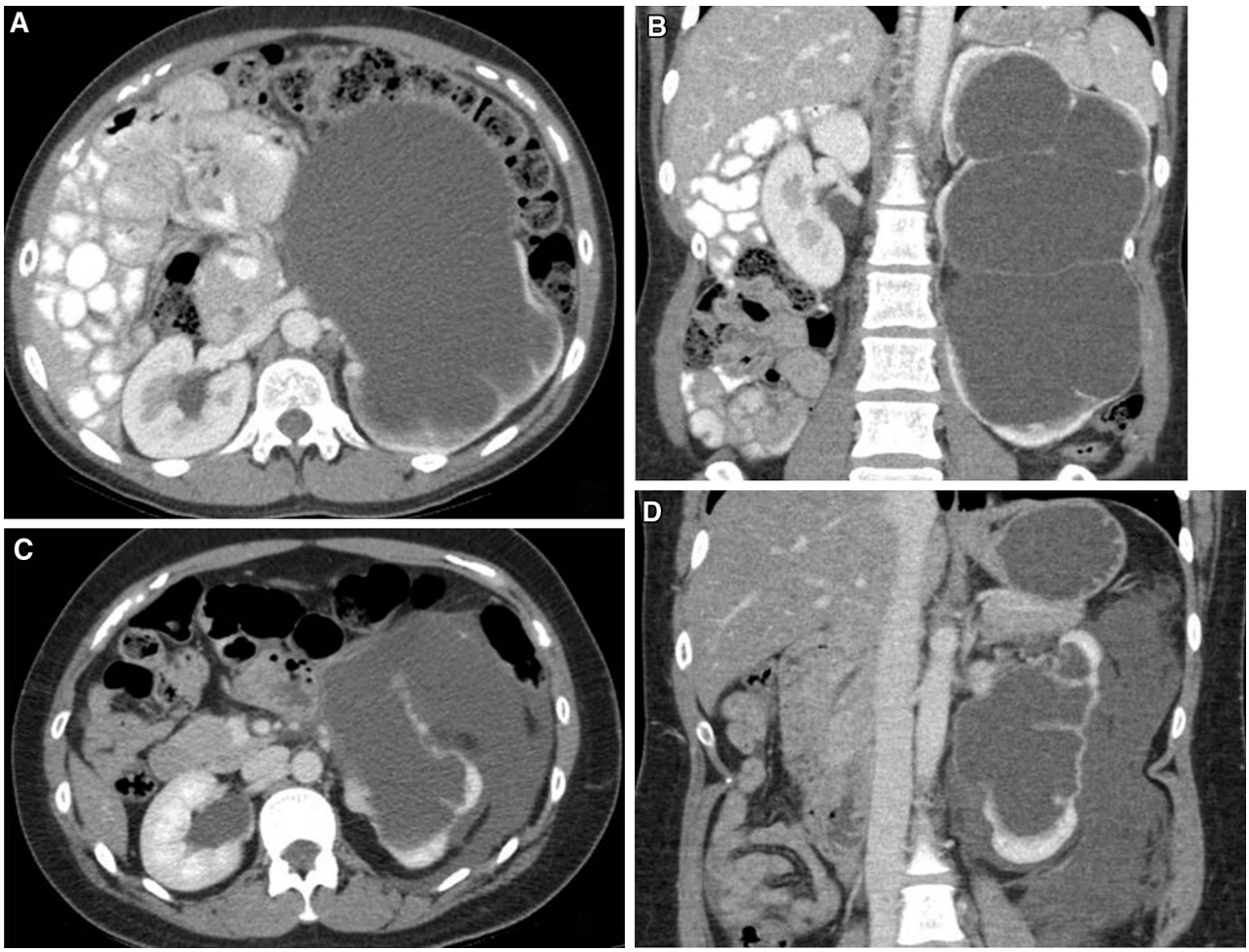

Fig. 33. Urinoma. **A**, **B** Large left renal urinoma. **C**, **D** Three years later, rupture of the urinoma, identifying extensive left perinephric free fluid.

Fig. 34. Lymphocele. Contrast-enhanced CT axial image shows a postoperative cystic lesion in left hemipelvis (*arrow*) related to a lymphocele secondary to recent surgery.

Fig. 35. Urachal cyst. **A** Axial, **B** sagittal T2-weighted MR image shows a small anterior rounded cystic lesion (*arrow*) between the umbilicus and the pubis related to a non-complicated urachal cyst.

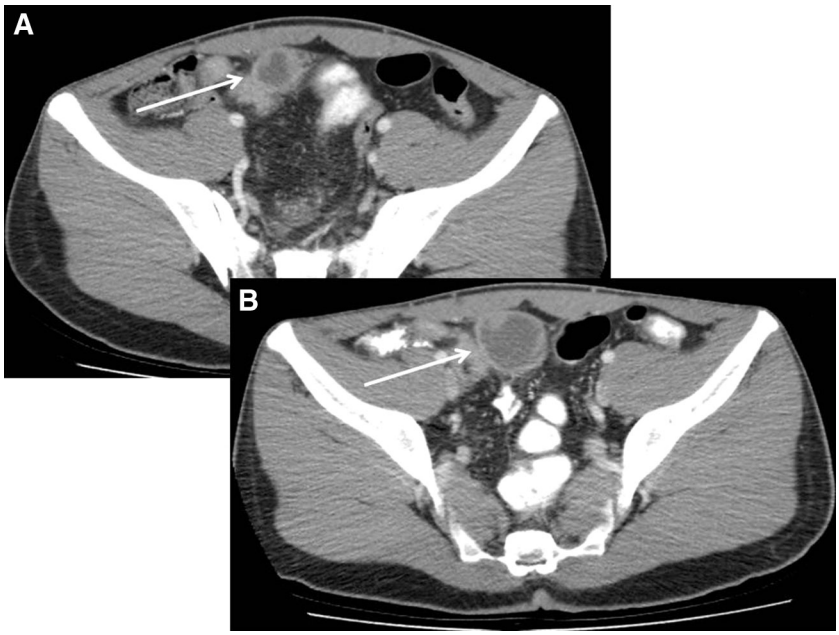

Fig. 36. Abscess. Patient with Crohn's disease. **A** Contrast-enhanced CT axial image shows a cystic thick-walled lesion in the hemipelvis (*arrow*) related to a small abscess. **B** Two months later interval enlargement of the abscess is demonstrated.

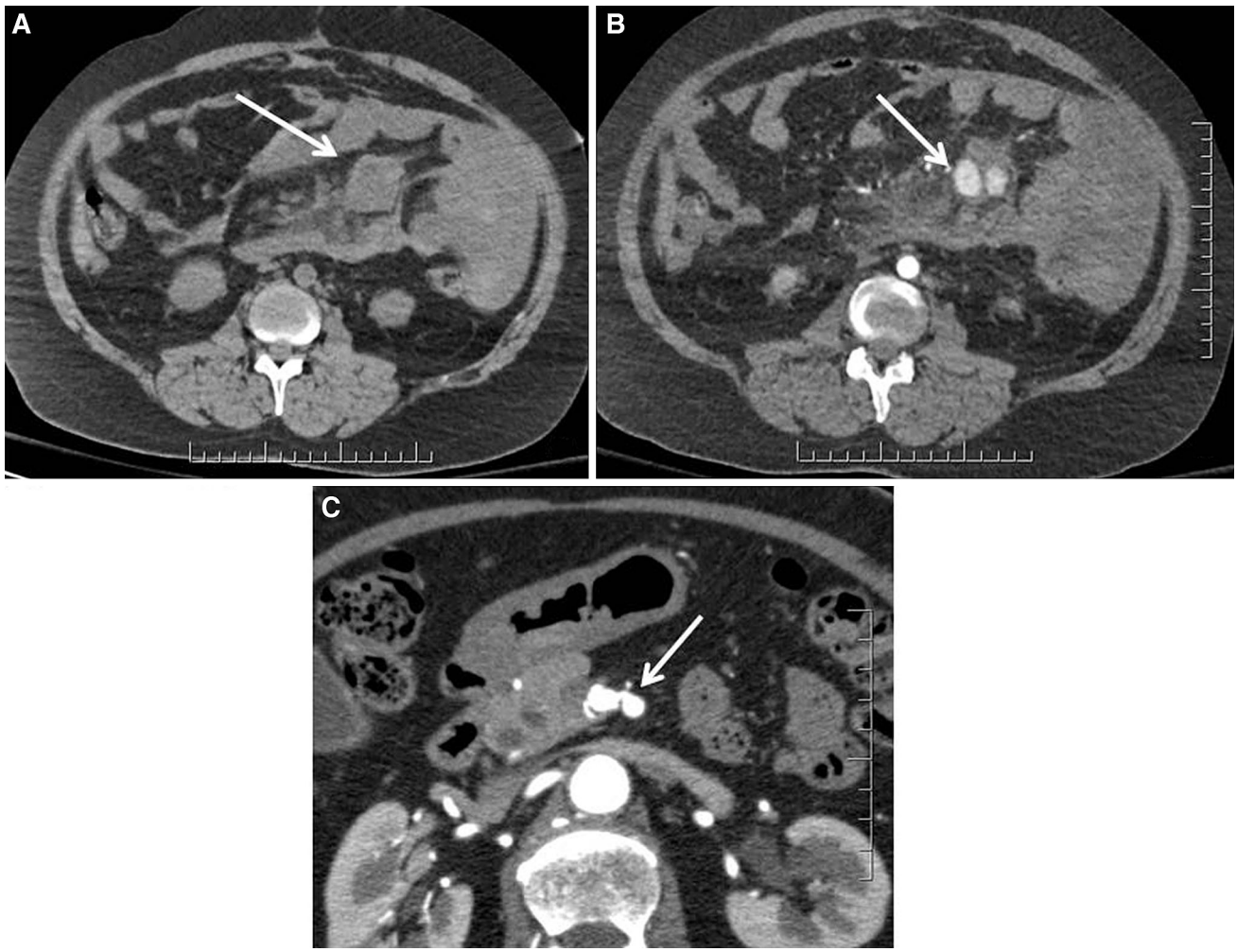

Fig. 37. Pseudoaneurysm and aneurysm of the superior mesenteric artery branches. **A** Axial non-enhanced CT shows a small cystic lesion in the left side of the mesentery (*arrow*) with increase of adjacent complex fluid. **B** After intravenous contrast a pseudoaneurysm of a superior mesenteric artery branch with adjacent bleeding is shown. **C** Axial contrast-enhanced CT shows a small superior mesenteric artery aneurysm (*arrow*).

Conclusion

Many of the primary cystic peritoneal masses have specific imaging features which can help in accurate diagnosis and management of these entities. Knowledge of the imaging spectrum of cystic peritoneal masses is necessary to distinguish them from other potential cystic abdominal mimickers masses.

Acknowledgments. The authors acknowledge Dr. Chavhan for images contribution.

References

1. Ros PR, Olmsted WW, Moser RP Jr, et al. (1987) Mesenteric and omental cysts: histologic classification with imaging correlation. Radiology 164(2):327–332
2. Stoupis C, Ros PR, Abbitt PL, Burton SS, Gauger J (1994) Bubbles in the belly: imaging of cystic mesenteric or omental masses. Radiographics 14(4):729–737
3. Tong SC, Pitman M, Anupindi SA (2002) Best cases from the AFIP. Ileocecal enteric duplication cyst: radiologic–pathologic correlation. Radiographics 22(5):1217–1222
4. Favara BE, Franciosi RA, Akers DR (1971) Enteric duplications. Thirty-seven cases: a vascular theory of pathogenesis. Am J Dis Child 122(6):501–506
5. Bremer JL (1944) Diverticula and duplications of the intestinal tract. Arch Pathol Lab Med 38:132–140
6. Otter MI, Marks CG, Cook MG (1996) An unusual presentation of intestinal duplication with a literature review. Dig Dis Sci 41(3):627–629
7. Dutheil-Doco A, Ducou Le Pointe H, Larroquet M, Ben Lagha N, Montagne J (1998) A case of perforated cystic duplication of the transverse colon. Pediatr Radiol 28(1):20–22
8. Lecouffe P, Spyckerelle C, Venel H, Meuriot S, Marchandise X (1992) Use of pertechnetate 99mTc for abdominal scanning in localising an ileal duplication cyst: case report and review of the literature. Eur J Nucl Med 19(1):65–67
9. Royal SA, Hedlund GL, Kelly DR (1994) Ileal duplication cyst. AJR Am J Roentgenol 163(1):98
10. Royle SG, Doig CM (1988) Perforation of the jejunum secondary to a duplication cyst lined with ectopic gastric mucosa. J Pediatr Surg 23(11):1025–1026
11. Rose JS, Gribetz D, Krasna IH (1978) Ileal duplication cyst: the importance of sodium pertechnetate Tc 99m scanning. Pediatr Radiol 6(4):244–246
12. Barr LL, Hayden CK Jr, Stansberry SD, Swischuk LE (1990) Enteric duplication cysts in children: are their ultrasonographic wall characteristics diagnostic? Pediatr Radiol 20(5):326–328
13. Levy AD, Cantisani V, Miettinen M (2004) Abdominal lymphangiomas: imaging features with pathologic correlation. AJR Am J Roentgenol 182(6):1485–1491
14. Lugo-Olivieri CH, Taylor GA (1993) CT differentiation of large abdominal lymphangioma from ascites. Pediatr Radiol 23(2):129–130
15. Davidson AJ, Hartman DS (1990) Lymphangioma of the retroperitoneum: CT and sonographic characteristic. Radiology 175(2):507–510
16. Mimura T, Kuramoto S, Hashimoto M, et al. (1997) Unroofing for lymphangioma of the large intestine: a new approach to endoscopic treatment. Gastrointest Endosc 46(3):259–263
17. Zhu H, Wu ZY, Lin XZ, et al. (2008) Gastrointestinal tract lymphangiomas: findings at CT and endoscopic imaging with histopathologic correlation. Abdom Imaging 33(6):662–668
18. Marom EM, Moran CA, Munden RF (2004) Generalized lymphangiomatosis. AJR Am J Roentgenol 182(4):1068
19. Wicks JD, Silver TM, Bree RL (1978) Giant cystic abdominal masses in children and adolescents: ultrasonic differential diagnosis. AJR Am J Roentgenol 130(5):853–857
20. Ko SF, Ng SH, Shieh CS, et al. (1995) Mesenteric cystic lymphangioma with myxoid degeneration: unusual CT and MR manifestations. Pediatr Radiol 25(7):525–527
21. Ayyappan AP, Jhaveri KS, Haider MA (2011) Radiological assessment of mesenteric and retroperitoneal cysts in adults: is there a role for chemical shift MRI? Clin Imaging 35(2):127–132
22. Vardy PA, Lebenthal E, Shwachman H (1975) Intestinal lymphangiectasia: a reappraisal. Pediatrics 55(6):842–851
23. Fox U, Lucani G (1993) Disorders of the intestinal mesenteric lymphatic system. Lymphology 26(2):61–66
24. Yang DM, Jung DH (2003) Localized intestinal lymphangiectasia: CT findings. AJR Am J Roentgenol 180(1):213–214
25. Persaud T, Swan N, Torreggiani WC (2007) Giant mucinous cystadenoma of the appendix. Radiographics 27(2):553–557
26. Fann JI, Vierra M, Fisher D, Oberhelman HA Jr, Cobb L (1993) Pseudomyxoma peritonei. Surg Gynecol Obstet 177(5):441–447
27. Hanbidge AE, Lynch D, Wilson SR (2003) US of the peritoneum. Radiographics 23(3):663–684; discussion 84–85
28. Yoo E, Kim JH, Kim MJ, et al. (2007) Greater and lesser omenta: normal anatomy and pathologic processes. Radiographics 27(3):707–720
29. Walkey MM, Friedman AC, Sohotra P, Radecki PD (1988) CT manifestations of peritoneal carcinomatosis. AJR Am J Roentgenol 150(5):1035–1041
30. Kawamoto S, Urban BA, Fishman EK (1999) CT of epithelial ovarian tumors. Radiographics 19(Spec No):S85–S102; quiz S263–S264
31. Jeong YY, Outwater EK, Kang HK (2000) Imaging evaluation of ovarian masses. Radiographics 20(5):1445–1470
32. Ghossain MA, Buy JN, Ligneres C, et al. (1991) Epithelial tumors of the ovary: comparison of MR and CT findings. Radiology 181(3):863–870
33. Pretorius ES, Outwater EK, Hunt JL, Siegelman ES (2001) Magnetic resonance imaging of the ovary. Top Magn Reson Imaging 12(2):131–146
34. Levy AD, Arnaiz J, Shaw JC, Sobin LH (2008) From the archives of the AFIP: primary peritoneal tumors: imaging features with pathologic correlation. Radiographics 28(2):583–607; quiz 21–22
35. Weiss SW, Tavassoli FA (1988) Multicystic mesothelioma. An analysis of pathologic findings and biologic behavior in 37 cases. Am J Surg Pathol 12(10):737–746
36. Ross MJ, Welch WR, Scully RE (1989) Multilocular peritoneal inclusion cysts (so-called cystic mesotheliomas). Cancer 64(6):1336–1346
37. Kim JS, Lee HJ, Woo SK, Lee TS (1997) Peritoneal inclusion cysts and their relationship to the ovaries: evaluation with sonography. Radiology 204(2):481–484
38. Schuetz MJ 3rd, Elsheikh TM (2002) Dermoid cyst (mature cystic teratoma) of the cecum. Histologic and cytologic features with review of the literature. Arch Pathol Lab Med 126(1):97–99
39. Sakurai Y, Uraguchi T, Imazu H, et al. (2000) Submucosal dermoid cyst of the rectum: report of a case. Surg Today 30(2):195–198
40. Vermeulen BJ, Widgren S, Gur V, et al. (1990) Dermoid cyst of the pancreas. Case report and review of the literature. Gastroenterol Clin Biol 14(12):1023–1025
41. Oray-Schrom P, St Martin D, Bartelloni P, Amoateng-Adjepong Y (2002) Giant nonpancreatic pseudocyst causing acute anuria. J Clin Gastroenterol 34(2):160–163
42. Fujita N, Noda Y, Kobayashi G, et al. (1995) Chylous cyst of the mesentery: US and CT diagnosis. Abdom Imaging 20(3):259–261
43. Yang DM, Jung DH, Kim H, et al. (2004) Retroperitoneal cystic masses: CT, clinical, and pathologic findings and literature review. Radiographics 24(5):1353–1365
44. Ilica AT, Kocaoglu M, Zeybek N, et al. (2007) Extrahepatic abdominal hydatid disease caused by *Echinococcus granulosus*: imaging findings. AJR Am J Roentgenol 189(2):337–343
45. Karavias DD, Vagianos CE, Kakkos SK, Panagopoulos CM, Androulakis JA (1996) *Peritoneal echinococcosis*. World J Surg 20(3):337–340
46. Harisinghani MG, McLoud TC, Shepard JA, et al. (2000) Tuberculosis from head to toe. Radiographics 20(2):449–470; quiz 528–529, 532
47. Gharbi HA, Hassine W, Brauner MW, Dupuch K (1981) Ultrasound examination of the hydatic liver. Radiology 139(2):459–463
48. Chiou SY, Sheu MH, Wang JH, Chang CY (2003) Peritoneal serous papillary carcinoma: a reappraisal of CT imaging features and literature review. Abdom Imaging 28(6):815–819

49. Furukawa T, Ueda J, Takahashi S, et al. (1999) Peritoneal serous papillary carcinoma: radiological appearance. Abdom Imaging 24(1):78–81
50. Park JY, Kim KW, Kwon HJ, et al. (2008) Peritoneal mesotheliomas: clinicopathologic features, CT findings, and differential diagnosis. AJR Am J Roentgenol 191(3):814–825
51. Stuart GC, Dawson LM (2003) Update on granulosa cell tumours of the ovary. Curr Opin Obstet Gynecol 15(1):33–37
52. Levy AD, Remotti HE, Thompson WM, Sobin LH, Miettinen M (2003) Gastrointestinal stromal tumors: radiologic features with pathologic correlation. Radiographics 23(2):283–304, 456; quiz 532
53. Miettinen M, Lasota J (2001) Gastrointestinal stromal tumors—definition, clinical, histological, immunohistochemical, and molecular genetic features and differential diagnosis. Virchows Arch 438(1):1–12
54. Fletcher CD, Berman JJ, Corless C, et al. (2002) Diagnosis of gastrointestinal stromal tumors: a consensus approach. Hum Pathol 33(5):459–465
55. King DM (2005) The radiology of gastrointestinal stromal tumours (GIST). Cancer Imaging 5:150–156
56. Yu JS, Kim KW, Lee HJ, et al. (2001) Urachal remnant diseases: spectrum of CT and US findings. Radiographics 21(2):451–461
57. MacNeily AE, Koleilat N, Kiruluta HG, Homsy YL (1992) Urachal abscesses: protean manifestations, their recognition, and management. Urology 40(6):530–535
58. Nagasaki A, Handa N, Kawanami T (1991) Diagnosis of urachal anomalies in infancy and childhood by contrast fistulography, ultrasound and CT. Pediatr Radiol 21(5):321–323